Institute für Theoretische Physik

Master Thesis

Investigation of a $\bar{b}\bar{b}ud$ tetraquark state, with quantum numbers $I(J^P) = 0(1^-)$, using lattice QCD static potentials

---

Author:
André Zimermmane Castro Santos

Supervisor:
Prof Dr. Marc Wagner

A thesis submitted in fulfillment of the requirements for the degree of Master of Science

October 19, 2020

Declaration of Authorship

Erklärung nach § 30 (12)Ordnung für den Bachelor- und dem Masterstudiengang

Hiermit erkläre ich, dass ich die Arbeit selbstständig und ohne Benutzung anderer als der angegebenen Quellen und Hilfsmittel verfasst habe. Alle Stellen der Arbeit, die wörtlich oder sinngemäß aus Veröffentlichungen oder aus anderen fremden Texten entnommen wurden, sind von mir als solche kenntlich gemacht worden. Ferner erkläre ich, dass die Arbeit nicht - auch nicht auszugsweise - für eine andere Prüfung verwendet wurde.

Frankfurt am Main, October 19, 2020

André Zimermmane Castro Santos

"*Science is a flirt with the unknown, a recognition that we know little of the world around us, which we can perceive only imperfectly. Yet, as it embraces the quest for knowledge, it lifts the human spirit and brings, through the joy of discovery, a touch of the magical in our lives.* "

Marcelo Gleiser

(Templeton Prize Acceptance Speech, May 2019)

Abstract

The study of exotic hadrons composed of four or more valence quarks is very challenging, both from a theoretical and a experimental perspective. Heavy-light tetraquark states composed of $\bar{b}\bar{b}ud$, although not being yet measured, have been a promising state, with predictions of bound sates and resonances occurring in the last years. Here, this particular system is further investigated under the Born-Oppenheimer approximation using static potentials computed from lattice-QCD. We obtain a framework including heavy spin corrections into the static approximation, which also comprises excited states of orbital angular momentum, extending previous studies. The main goal is to access their effects on a resonance with quantum numbers $I(J^P) = 0(1^-)$. A coupled channel of BB and B^*B^* meson pairs is suggested as the main contributor to such state. Their non-relativistic-quantum-mechanical phase-shifts and T matrix eigenvalues indicates that such resonance could be suppressed by $\bar{b}\bar{b}$ spin effects. Further future analysis, taking into account the uncertainties in the potentials and going above the $2m_{B^*}$ mass threshold would be valuable for a broader picture.

Contents

Chapter 1

Introduction

The proposal of the constituent quark model, developed independently by Gellman [1] and Zweig [2] in 1964, has provided a successful description of hadrons in terms of colour neutral three-quark (barions) and quark-antiquark (mesons) bound states. These seminal works did not exclude the existence of more exotic quark combinations mathematically, such as tetraquarks and pentaquarks, although they were not observed in nature. As early as in 1977, a spectrum for multiquarks states was proposed by Jaffe [3] in an innovative study using the bag model [4] to confine coloured quarks and gluons, as required in perturbative *Quantum Chromodynamics* (*QCD*). Still, a theoretical description of exotic hadrons has been shown very challenging [5–9] and a complete picture is missing. Nevertheless, their understating is not only fundamental for a full comprehension of the binding mechanisms of *QCD* [10]. Due to the fact that they have been hypothesised to naturally form in extreme conditions, such as in the core of neutron stars [11], their understating can also contributes to the better comprehension of the matter constitution in the universe.

From the experimental side, the quest non conventional handrons is not less demanding. Difficulties arise, particularly, as a result of the high hadronic spectrum in which they are located and their fast decay rate to non-exotic hadrons. Consequently, the first clear experimental hint of a particle not obeying the standard hadronic classification, the hence called $X(3872)$, was only detected in 2003 by the Belle experiment [12], with almost 40 years gap from the pioneering introductions of the quark model. The peculiar state, having *charm* quarks but a mass that did not agree with the spectrum of the charmomium ($c\bar{c}$) is the first tetraquark candidate ever measured [13]. From then, instigating observations followed. For instance, the *BaBar* Collaboration measured $Y(4260)$ [14], which explanation is still subject of theoretical investigations [15], and the unambiguous exotic $Z(4430)$ claimed by Belle [16] and LHCb [17]. Hence, the era of the XYZ particle discoveries was inaugurated, re-sparkling theoretical interest in multi-quark matter. Possible explanations ranged from molecular mesonic states, tetraquark states, hadron-charmonium, hybrid states (charmonium states with an extra gluon) and even models of initial single-pion emission.

Among the dozens of exotic Standard Model hadrons that surged since then, only a few are corroborated successfully by theory as four quark systems. This is the case of, but not exclusively, the double-heavy quark classes $Z_b^{\pm}$, a $bq\bar{b}\bar{q}$ state and the $Z_c(3900)$, a $cq\bar{c}\bar{q}$) state, that were claimed by BELLE[18] and BESIII [19], respectively. It is also the situation of the most recent measurement of $X(6900)$, the first seen system with four heavy quarks ($cc\bar{c}\bar{c}$) claimed by *LHCb* [20]. In lattice *QCD* challenges arise not only from the choice of the relevant structures in the creation operators, but also from the fact that many states are QCD resonances well above the threshold. As a result, they contain many lighter decay channels [21]. On the other hand, quark model calculations depend highly on the choice of potentials. One example is the

string flip-flop potential for meson-meson interaction [5–8], which has been shown to result in an exaggerated binding [22].

In this work, tetraquarks are analysed from an alternative approach, which combines techniques from lattice QCD and quantum mechanics to circumvent complications arising from pure lattice QCD. Focus is given to a promising $ud\bar{b}\bar{b}$ state, which is related to the observed $Z_b^{\pm}$, but has the theoretical advantage of having less decay channels. In spite of the fact that systems containing two heavy antiquarks are more problematic to generate and detect experimentally, hence not being measured yet, their stability has been studied systematically in theory [23–27]. The hybrid approach that will be considered relies on the determination of lattice QCD potentials for two static heavy antiquarks $\bar{b}\bar{b}$ in the presence of two light quarks ud. The static approximation implies that $\bar{b}\bar{b}$ are infinitely heavy and their spin irrelevant. By means of a Born-Oppenheimer approximation, such potentials are included in a quantum mechanical Hamiltonian, allowing wave function determinations. Such strategy has previously suggested the existence of $ud\bar{b}\bar{b}$ bound states with quantum numbers $I(J^P) = 0(1^+)$ [28–30], which persisted even when corrections from heavy spin were added [31]. Their final binding energy was estimated to $m_{\mathrm{B}} = 10545^{+30}_{-38}$ MeV. Furthermore, it has also indicated a resonances $I(J^P) = 0(1^-)$ with mass $m_{\mathrm{R}} = 10576^{+4}_{-4}$ MeV [32]. However, for the latter, the more convoluted effects from heavy spins were not regarded.

It is well known that $\bar{b}\bar{b}$ spin are not negligible. They manifest in the mass difference of B mesons, $m_{B^*} - m_B \approx 45$ MeV, which would be degenerate otherwise. Such mass splitting is, in fact, of the same order of magnitude as the binding and resonance energies previously found. Additionally, spin effects are expected to weaken both, binding and resonance energies of the system. For this reason, in this work, we aim at investigating the effects on excited states of $ud\bar{b}\bar{b}$, with a particular interest on the resonance $I(J^P) = 0(1^-)$. For doing so, a necessary formalism to include excited states in the analysis will be developed, generalising a similar approach performed in a previous study for a bound states analysis [31]. We start, in Chapter 2, describing the approach used to treat multi-channel heavy-light tetraquarks in the Born-Oppenheimer approximation. Symmetries and quantum numbers are, thus, thoroughly analysed in Chapter 3, in order to to account for arbitrary orbital angular momentum states. Next, Chapters 4 and 5 concern, respectively, with bound state and resonances studies of the relevant contribution for $I(J^P) = 0(1^-)$. Finally, conclusion and perspectives are presented in Chapter 5.

Chapter 2

Heavy-light tetraquarks formalism

The description of heavy-light tetraquark states in this work relies in an approach containing two steps. First, one considers lattice *QCD* static potentials computed for two heavy anti-quarks $\bar{Q}\bar{Q}$ in the presence of two light quarks, qq. Later, the Born-Oppenheimer approximation is utilised, in order to set a Schrödinger equation for the heavy-degrees of freedom.

2.1 Static lattice *QCD* Potentials for $\bar{Q}\bar{Q}qq$

In the static approximation of lattice *QCD*, the effective potentials of a pair of heavy anti-quarks $\bar{Q}\bar{Q}$ immersed in a cloud of two light quarks $q \in \{u, d\}$ can be determined for a spatial separation $r = |\mathbf{r}_2 - \mathbf{r}_1|$ using the following four-quark creation operators:

$$\mathcal{O}_{\mathbb{L},\mathbb{S}}(r) = (\mathcal{C}\mathbb{L})_{\alpha\beta}(\mathcal{C}\mathbb{S})_{\gamma\delta}\Big(\bar{Q}^a_\gamma(\mathbf{r_1})q^{(f)a}_\alpha(\mathbf{r_1})\Big)\Big(\bar{Q}^b_\delta(\mathbf{r_2})q^{(f')b}_\beta(\mathbf{r_2})\Big)\ , \tag{2.1}$$

where a, b denote colour indices, α, β, γ, δ denote spin and f,f' are related to the isospin. The matrices terms are the charge conjugation $\mathcal{C} = \gamma_0\gamma_2$, the spin coupling of the satic antiquark $\mathbb{S}$ and, finally, the spin coupling of the light quarks $\mathbb{L}$. Additionally, there are symmetric and antisymmetric possibilities in according to isospin I:

$$q^{(f)}q^{(f')} = \begin{cases} \frac{1}{\sqrt{2}}(ud - du) & \text{for } I = 0 \\ uu,\ \frac{1}{\sqrt{2}}(ud + du),\ dd & \text{for } I = 1 \end{cases}\ , \tag{2.2}$$

In the static approximation the heavy antiquarks are infinitely heavy. Formally, that means that their position $\mathbf{r}_1, \mathbf{r}_2$ are fixed. This bring two implications: the potentials do not depend on the heavy spins and the total heavy spin and total light spin are conserved separately. The latter makes appropriated the coupling of the two heavy spins via $\mathbb{S}$ and the two light spins via $\mathbb{L}$.

The heavy quarks, being fully non-relativistic, contain only two spin components in their spinors, while the light quarks are fully relativistic. This is realised via the transformation $\bar{Q} \longrightarrow \bar{Q}(\mathbb{1} + \gamma_0)/2$. As a consequence, there are 8 spin coupling possibilities, for $\mathbb{S}$ and $\mathbb{L}$, each, corresponding to combinations of γ matrices that are linear independent between themselves. They are

$$\mathbb{L}, \mathbb{S} \in \{\ (\mathbb{1} + \gamma_0)\gamma_5,\ (\mathbb{1} + \gamma_0)\gamma_j,\ (\mathbb{1} + \gamma_0)\mathbb{1},\ (\mathbb{1} + \gamma_0)\gamma_j\gamma_5\ \} \quad \text{for } j = 1, 2, 3\ ,$$

In the static approximation the lattice *QCD* potentials generated, only depend on the coupling $\mathbb{L}$. In this work, as we shall see in detail the next chapter, we will focus on a subgroup of the potentials giving light spin $s_{qq} = 0$ and $s_{qq} = 1$ obtained with

the couplings

$$\mathbb{L} = \begin{cases} (\mathbb{1}+\gamma_0)\gamma_5 \longrightarrow V_5(r) & \text{for } s_{qq}=0\ , \\ (\mathbb{1}+\gamma_0)\gamma_j \longrightarrow V_j(r) & \text{for } s_{qq}=1\ . \end{cases} \tag{2.3}$$

where $r = |\mathbf{r}_2 - \mathbf{r}_1|$. Due the fact that those potentials are independent on the heavy spin, for each $\mathbb{L}$ the corresponding potentials are obtained by an arbitrary choice of $\mathbb{S}$.

After operators are set with the relevant quantum numbers, one can use standard methods of lattice *QCD* [33] to calculate the correlation functions with temporal separation t

$$C(t,r) = \langle\Omega|\mathcal{O}^{\dagger}_{\mathbb{L},\mathbb{S}}(t,r)\mathcal{O}_{\mathbb{L},\mathbb{S}}(0,r)|\Omega\rangle \tag{2.4}$$

from where the potentials can be extracted from the asymptotic exponential decay of $C(t,r)$.

By means of (2.4), the potentials are obtained from first principles in the static limit $1/m_b \to 0$, but rather for a finite number of discrete separations r. In order to have a continuous description, which will allow their incorporation into non-relativistic quantum mechanical Schrödinger equations, a fit to the lattice QCD data is necessary. The appropriated fit function is based on the qualitative behaviour of the four quark system's interaction. For small separations, the heavy antiquarks form an antidiquark, being dominated by a gluon-exchange potential, which is Coulomb-like. On the other hand, at large separations the light u/d quarks introduce screening and, thus, the system forms two interacting heavy-light mesons(*c.f.* Figure 2.1). For this reason, a screened Coulomb potential is used as fit anzats

$$V_x(r) = \pm\frac{\alpha_x}{r}\mathrm{e}^{-(r/d_x)^2} + V_0 \tag{2.5}$$

where V_0 is a term accounting for twice the mass of the heavy-light mesons, namely, the asymptotic value for $r \to \infty$. The coupling α_x and the range d_x are parameters determined from the fit, where $x = 5, j$. The signs are $-$ for attractive and $+$ for repulsive potentials depending, essentially, on the colour state of the heavy quarks as will be discussed in more detail in Section 3.2.1. Finally, in order to quantify systematic errors fits are typically performed for different temporal separations $t_{\min} < t < t_{\max}$ of the correlation function $C(t,r)$ where $V_x(r)$ are read off and for several spatial separations $r_{\min} < r < r_{\max}$.

In this work, available lattice computed potentials of $\bar{b}\bar{b}$ in the presence of the light u/d will be used [33]. In [30], fits for different heavier-than-physical pion masses and a subsequent extrapolation provided α_5 and d_5 at the physical point for the attractive cases ($s_{qq}=0$, $I=0$) and ($s_{qq}=1$, $I=1$). For the repulsive ones, the statistical uncertainties were much larger and, for this reason, a precise stable quark mass extrapolation was not possible. Nonetheless, a consistent parametrization of the lattice QCD data with errors estimated conservatively, allowed an determination of α_j and d_j for ($s_{qq}=1$, $I=0$), as presented in [31]. The parameter of the $I=0$ potentials utilised further in this work are presented in Table 2.1 and a visualisation is available as a plot in Figure 2.2.

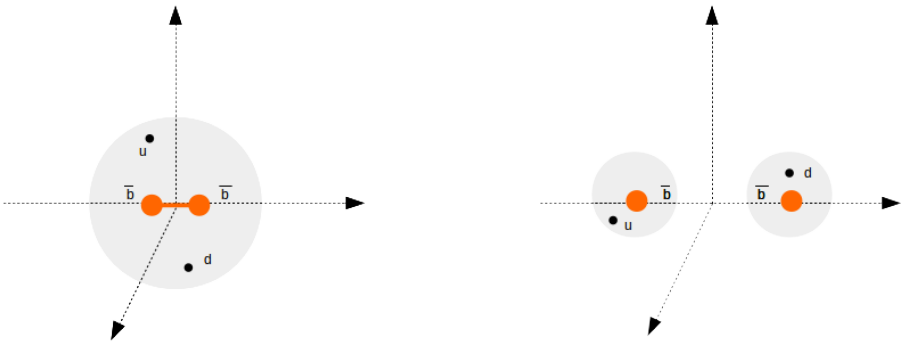

(A) (B)

FIGURE 2.1: Picture of a $\bar{b}\bar{b}ud$ system. (A) At small $\bar{b}\bar{b}$ separations of the heavy antiquarks interact via gluon-exchange, forming a heavy antidiquark. (B) At larger separations, screening from the light quarks become relevant and the system forms two interacting heavy-light mesons.

s_{qq}	α	d (fm)
0	$0.34^{+0.03}_{-0.03}$	$0.45^{+0.12}_{-0.10}$
1	$0.10^{+0.07}_{-0.07}$	$0.28^{+0.17}_{-0.17}$

TABLE 2.1: Potential parameters for $I = 0$ available from fits performed in [30, 31]

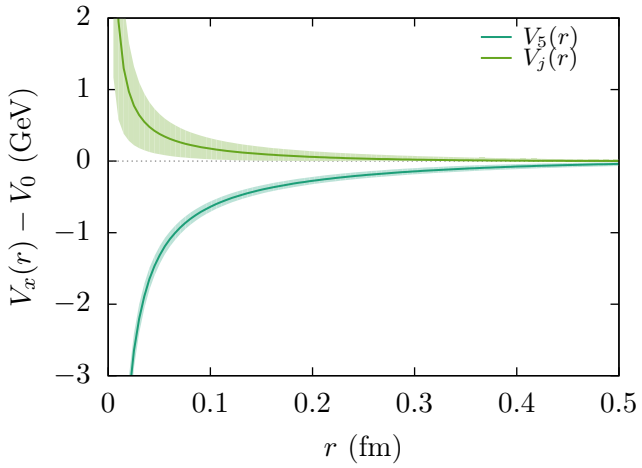

FIGURE 2.2: Plot of the $I = 0$ attractive V_5 and repulsive V_j potentials as a function of $\bar{b}\bar{b}$ separation r. Solid lines are the mean values, while filled lines represent the uncertainties in according to the parametrisation shown in Table 2.1.

2.2 The Born-Oppenheimer Approximation

The dynamics of the system is introduced via the Born-Oppenheimer approximation. The approach is analogous to the molecular dynamics methods, where the heavy

degrees of freedom $\bar{b}\bar{b}$, analogous to protons in a hydrogen molecule, are treated separately from the light degrees of freedoms u/d, which, in this case, are 'electrons' with special properties.

The lattice *QCD* determination of the light-spin-dependent effective potential $V_{\mathbb{S}}$ of the $\bar{b}\bar{b}$ pair immersed in a cloud of light u/d is the first step of the approximation. Next, this potential is embedded in the system's Hamiltonian, in order to set a two-body Schrödinger equation for $\bar{b}\bar{b}$ [1]:

$$\left(-\frac{1}{2m_b}\nabla^2 + V_{\mathbb{S}}(r)\right)\Psi(\mathbf{r}_1,\mathbf{r}_2) = E\Psi(\mathbf{r}_1,\mathbf{r}_2)\ . \tag{2.6}$$

This stationary Schrödinger equations is precisely the second step of the Born-Oppenheimer approximation. It can be solved for bound states by procuring energy eigenvalues. When existent, they are related to the masses of the strongly bound four-quark system. Furthermore, one can use the scattering theory's emergent wave method to search for resonances. It is important to remark, however, that because the potentials are independent of $\bar{b}\bar{b}$ spins, the effects of the couplings between heavy and light spin continue to be totally neglected.

2.3 Interpreting lattice *QCD* potentials in terms of B and B^* mesons

In order to understand how one can introduce heavy spin corrections to the system, first, it is necessary to understand how the heavy-light tetraquarks can be described in terms of their asymptotic behaviour, *i.e.* in terms of interacting heavy-light meson pairs. As previously mentioned at larger separations, the strongly bound system is weakened by light u/d quarks screening and, for this reason, the four quarks form rather two interacting B mesons (Figure 2.1). Based on that, one can let explicit the meson-meson structure by a special reordering of the creation operators on (2.1). For doing so, the linear transformation that allows one to express them in terms of static-light bilinears of the form $\bar{Q}\Gamma q$ needs to be found.

2.3.1 The Fierz identities

This transformations can be constructing using the Fierz identities[34], relations commonly used to study four-fermion operators. They are particularly useful for rewriting products of two bilinears as linear combinations of products of different bilinears, allowing the reordering of the Dirac spinors.

They are based on the fact that the standard Dirac γ matrices[35] have sixteen product combinations

$$\Gamma^a \in \{\mathbb{1}\ ,\gamma^\mu\ ,\sigma^{\mu\nu}\ ,i\gamma^\mu\gamma_5\ ,\gamma_5\} \quad (\mu,\nu = 0,1,2,3)\ , \tag{2.7}$$

where

$$\sigma^{\mu\nu} = \frac{i}{2}[\gamma^\mu,\gamma^\nu] \quad \text{with} \quad (\mu<\nu)\ , \tag{2.8}$$

$$\gamma_5 = \gamma^5 = i\gamma^0\gamma^1\gamma^2\gamma^3\ . \tag{2.9}$$

[1] In this study we follow the high-energy physics practice of working with Natural Units ($\hbar = c = 1$).

Note that each Γ^a gives an specific behaviour to the corresponding bilinears $\bar{\psi}\Gamma^a\psi$ with respect to Lorentz transformations. Furthermore, Γ^a's have the property of being linearly independent, spanning the sixteen dimensional space of all 4×4 complex matrices $\mathbb{C}^{4\times4}$. Indeed, they form a basis for this space with scalar product given by the trace of the product of two Γ^a.

Hence, considering Γ_a as the corresponding matrix with the space-time indices lowered by Minkowski metric, the orthogonality relation reads

$$\frac{1}{4}\mathrm{Tr}(\Gamma_a\Gamma^b) = \delta_a^b \ . \tag{2.10}$$

It follows that an arbitrary matrix $\mathrm{M} : \mathbb{C}^{(4\times4)} \to \mathbb{C}^{(4\times4)}$ can be then expanded as

$$\mathrm{M} = \frac{1}{4}\sum_a \mathrm{Tr}(\Gamma_a M)\Gamma^a \ . \tag{2.11}$$

Note that this arbitrary matrix can even be one of the specific Γ_a's. Finally, using (2.10) in the relation above, the completeness relation follows

$$\frac{1}{4}\sum_a (\Gamma^a)_{\alpha\beta}(\Gamma_a)_{\delta\gamma} = \delta_{\alpha\gamma}\delta_{\beta\delta} \ , \tag{2.12}$$

where Dirac indices $\alpha \cdots \gamma$ where let explicit.

These properties can be used to show that an arbitrary bi-product of bilinears, which contains four spinors $\bar{\psi}_1$,ψ_2 ,$\bar{\psi}_3$, ψ_4 and two coupling matrices Γ^a,Γ^b, can be represented as a linear superposition of variants with a changed sequence of spinors:

$$(\bar{\psi}_1\Gamma^a\psi_2)(\bar{\psi}_3\Gamma^b\psi_4) = \sum_{c,d} C_{cd}^{ab}(\bar{\psi}_1\Gamma^c\psi_4)(\bar{\psi}_3\Gamma^d\psi_2) \ , \tag{2.13}$$

where the coefficients

$$C_{cd}^{ab} = \frac{1}{16}\mathrm{Tr}\Big\{(\Gamma^a\Gamma_c\Gamma^b\Gamma_d)\Big\} \tag{2.14}$$

can be determined with the help of the completeness relations (2.12) [2]

In the static approximation, the static spinors $\bar{Q}$ have only two spin components, as discussed previously. Therefore, a new set of Γ-matrices is constructed spanning the sub-space of $\mathbb{C}^{4\times4}$ appropriated to describe bilinears containing $\bar{Q}$. This set is precisely the set of the couplings $\mathbb{L}$ and $\mathbb{S}$, as derived in [37]. Hence, they correspond to eight linear independent Γ^a's. Using Γ^a's to construct bilinears of the from $\bar{Q}\Gamma^a q$, provides an interpretation in terms of the meson contents

$$\Gamma^a = \begin{cases} (\mathbb{1}+\gamma_0)\gamma_5 & \text{for } J^P = 0^- \ (B \text{ meson}) \\ (\mathbb{1}+\gamma_0)\gamma_j & \text{for } J^P = 1^- \ (B^* \text{ meson}) \\ (\mathbb{1}+\gamma_0)\mathbb{1} & \text{for } J^P = 0^+ \ (B_0^* \text{ meson}) \\ (\mathbb{1}+\gamma_0)\gamma_j\gamma_5 & \text{for } J^P = 0^+ \ (B_1^* \text{ meson}) \end{cases} \ . \tag{2.15}$$

[2] For a simple derivation and detailed discussion refer to [36].

One can represent the heavy-light tetraquark creation operators (2.1) with their meson-meson structure explicit. They become

$$\mathcal{O}_{\mathbb{L},\mathbb{S}}(r) = \sum_{a,b} G(\mathbb{L},\mathbb{S})_{ab}\Big(\bar{Q}_{(}\mathbf{r_1})\Gamma^a q^{(f)}(\mathbf{r_1})\Big)\Big(\bar{Q}_{(}\mathbf{r_2})\Gamma^b q^{(f')}(\mathbf{r_2})\Big)\ , \tag{2.16}$$

where the coefficients

$$G(\mathbb{L},\mathbb{S})_{ab} = \frac{1}{16}\mathrm{Tr}\big((\mathcal{C}\mathbb{S})^T\Gamma_a^T(\mathcal{C}\mathbb{L})\Gamma_b\big) \tag{2.17}$$

are defined by the corresponding Fierz identity derived in [37].

2.3.2 The Coupled Channel Schrödinger Equation

Writing a Schrödinger Equation in the Born-Oppenheimer approximation with wave functions having meson pairs combination of B/B^* mesons as degrees of freedom is strategical. The reason for this is that it allows including heavy spin effects via the addition of B/B^* mass terms as asymptotic values for the potentials[31]. The relation between the wave function and the static potentials can then be found via (2.16).

Denoting $B^aB^b(\mathbf{r}_1,\mathbf{r}_2)$ as the wave function of B/B^* pairs constructed via the operators $\big(\bar{Q}_{(}\mathbf{r_1})\Gamma^a q^{(f)}(\mathbf{r_1})\big)\Big(\bar{Q}_{(}\mathbf{r_2})\Gamma^b q^{(f')}(\mathbf{r_2})\Big)$ and denoting $\psi_{\mathbb{SL}}(\mathbf{r}_1,\mathbf{r}_2)$ as the wave function obeying a Schrödinger equation of type (2.6), they can be related by

$$\psi_{\mathbb{SL}}(\mathbf{r}_1,\mathbf{r}_2) = \sum_{a,b} G(\mathbb{S},\mathbb{L})_{ab}\ B^aB^b(\mathbf{r}_1,\mathbf{r}_2) \tag{2.18}$$

In this study, only the lightest B mesons, B and B^* , are considered. One can shown via (2.16) that there are only sixteen possibilities of light and heavy spin couplings [37]

$$\mathbb{L},\mathbb{S} \in \{\ (\mathbb{1}+\gamma_0)\gamma_5,\ (\mathbb{1}+\gamma_0)\gamma_j\ \} \quad \text{for } j=1,2,3$$

giving $G(\mathbb{S},\mathbb{L})_{ab} \neq 0$. We introduce now the notation

$$B^a = \begin{cases} B & \text{if } \Gamma^i = (\mathbb{1}+\gamma_0)\gamma_5\ , \\ B_1^* & \text{if } \Gamma^i = (\mathbb{1}+\gamma_0)\gamma_1\ , \\ B_2^* & \text{if } \Gamma^i = (\mathbb{1}+\gamma_0)\gamma_2\ , \\ B_3^* & \text{if } \Gamma^i = (\mathbb{1}+\gamma_0)\gamma_3\ , \end{cases} \tag{2.19}$$

and write a vector $\Psi_{B^aB^b}$ having as entries each of the sixteen $B^aB^b(\mathbf{r}_1,\mathbf{r}_2)$ possible combinations as

$$\Psi_{B^aB^b} = \begin{pmatrix} BB \\ BB_1^* \\ \vdots \\ B_1^*B \\ B_1^*B_1^* \\ \vdots \\ B_3^*B_2^* \\ B_3^*B_3^* \end{pmatrix}\ . \tag{2.20}$$

By also defining a sixteen dimensional vector $\Psi_{\mathbb{SL}}$ having as entries the wave functions $\psi_{\mathbb{SL}}$, one reads

$$\Psi_{\mathbb{SL}} = \mathbb{G}\Psi_{B^aB^b} \ , \tag{2.21}$$

where the elements of the transformation matrix $\mathbb{G}$ are the coefficients $G(\mathbb{S},\mathbb{L})_{ab}$ organised in lines with indices $\mathbb{S},\mathbb{L}$ and columns with indices a,b.

From (2.21) it is straightforward to see that, giving a Schrödinger Equation for the heavy-light degrees of freedom, one can write a corresponding equation for the B/B^* pairs degrees of freedom by $\mathbb{G}^{-1}$ transforming it

$$H_{\mathbb{SL}}\ \Psi_{\mathbb{SL}} = E\ \Psi_{\mathbb{SL}} \quad \Leftrightarrow \quad H_{\mathbb{SL}}\ (\mathbb{G}\Psi_{B^aB^b}) = E\ (\mathbb{G}\Psi_{B^aB^b}) \tag{2.22}$$

$$\xrightarrow{G^{-1}} (\mathbb{G}^{-1}H_{\mathbb{SL}}\mathbb{G})\ \Psi_{B^aB^b} = E\ \Psi_{B^aB^b} \ . \tag{2.23}$$

It is clear from the Hamiltonian in (2.23) that the relation between the lattice computed static potentials, which are diagonal at (2.22), to the effective potentials of the B/B^* combinations is given by

$$\mathbb{G}^{-1}V_{\mathbb{SL}}\mathbb{G} \ . \tag{2.24}$$

In fact, the same conclusion could be obtained from the fact that the potentials are related to (2.16). Therefore, by arranging the light spin dependent potentials in the matrix

$$V_{\mathbb{SL}} = \mathrm{diag}(V_5(r), V_j(r), V_j(r), V_j(r)) \otimes \mathbb{1}_{4\times4} \ , \tag{2.25}$$

which is constructed to match the the linear combinations of B/B^* pairs given by $\Psi_{\mathbb{SL}}$, equation (2.24) gives the effective potentials of each B/B^* pair. They are a linear combination of V_5 and $V_j(r)$, resembling an interaction term that coupling the resulting Schrödinger equation. We define them by

$$H_{\mathrm{int}} = \mathbb{G}^{-1}V_{\mathbb{SL}}(r)\mathbb{G} \ , \tag{2.26}$$

Now all ingredients to write a Schrödinger Equation having the meson-meson structures are present. For elucidating purposes, the Hamiltonian is always expressed here separated in the free and interacting parts. The free part contains the kinetic term and the masses of the B/B^* pairs, the latter being the asymptotic values of the potentials accounting for the heavy spin corrections. Defining

$$M \equiv \mathrm{diag}(m_B, m_{B^*}, m_{B^*}, m_{B^*}) \ , \tag{2.27}$$

the free part reads

$$H_0 = M \otimes \mathbb{1}_{4\times4} + \mathbb{1}_{4\times4} \otimes M + \frac{\mathbf{p_1}^2}{2m_b} + \frac{\mathbf{p_2}^2}{2m_b} \ , \tag{2.28}$$

where the tensor structures $M \otimes \mathbb{1}_{4\times4} + \mathbb{1}_{4\times4} \otimes M$ accounts for the B/B^* masses $(2m_B\ ,\ m_B + m_{B^*}\ ,\ \cdots, 2m_{B^*})$ in the proper order.

Hence, the 16×16 coupled-channel two-body stationary Schrödinger equation is given by

$$[H_0 + H_{\mathrm{int}}]\Psi_{B^aB^b}(\mathbf{r}_1, \mathbf{r}_2) = E\Psi_{B^aB^b}(\mathbf{r}_1, \mathbf{r}_2) \ . \tag{2.29}$$

Chapter 3

Excited states of orbital angular momenta

This chapter concerns in setting the framework necessary for the search for excited states of angular momentum in the sixteen coupled Schrödinger equation derived (2.29). This step allows a posterior investigation of bound state and resonances. Before doing so, there are some further useful simplifications necessary. The first is to split the two-body Schrödinger Equation in two independent equations by doing a change of variables

$$\mathbf{r} = \mathbf{r}_1 - \mathbf{r}_2 \ , \tag{3.1}$$

$$\mathbf{r}_{\rm CM} = \frac{m_b}{2}(\mathbf{r}_1 + \mathbf{r}_2) \ , \tag{3.2}$$

where $\mathbf{r}$ is the relative coordinate and $\mathbf{r}_{\rm CM}$ is the centre of mass coordinate, a common procedure in ordinary quantum mechanics[1]. Such variable transformation works well because the resulting equation is separable. In fact, the equation for $\mathbf{r}_{\rm CM}$ corresponds to a free Schrödinger equation for the centre of mass wave functions. They have the free particle eingenstates coming from to the 'motion' of the centre of mass, being uninteresting for this study. On the other hand, the equation for $\mathbf{r}$ contains the information of the interaction, namely, possible bound and resonance states and, for that reason, we study it closely.

After performing such change of variables in equation (2.29) and writing the momentum operator explicitly in terms of the relative orbital angular momentum L, the relative coordinate equation reads

$$\left[M \otimes \mathbb{1}_{4\times4} + \mathbb{1}_{4\times4} \otimes M - \frac{1}{2\mu}\left(\frac{\partial^2}{\partial r^2} + \frac{2}{r}\frac{\partial}{\partial r} - \frac{\mathbf{L}^2}{r^2}\right)\mathbb{1}_{16\times16} + H_{\rm int}(r)\right]\Psi(\mathbf{r}) = E\Psi(\mathbf{r}) \ , \tag{3.3}$$

where $\mu = m_b/2$ is the reduced mass and Ψ is a vector having as entries the sixteen B/B^* pair combinations wave functions in the relative coordinate. Note that from now on, the subscript B^aB^b is omitted in Ψ, because only this type of wave functions will be utilised further in the work.

3.1 Symmetries and Quantum Numbers

Equation (3.3), although containing all the coupled channels for B/B^* pairs, is unpractical. The reason is as follows: four-quark states with different quantum numbers, more specifically, with different parity P and total angular momentum J, are coupled and share the same eigenvalues there. The situation becomes even more evolved when

[1] See, for example, section 15.4 in [38]

one considers excited states of orbital angular momentum. They, in principle, can introduce further possibilities of couplings and allowed states. For this reason, they were avoided in a previous studies.

In order to try to include them, the symmetries of the problem are analysed thoroughly at this section. Due to the consideration of excited states of orbital angular momentum for the first time in this system, it is insightful to look first at orbital angular momentum conservation.

3.1.1 Relative orbital angular momentum

Orbital angular momentum is conserved in quantum mechanics if one of the following conditions is satisfied

$$[\mathbf{L}^2, H] = 0 \ , \tag{3.4}$$
$$[L_z, H] = 0 \ . \tag{3.5}$$

In fact, if one of them holds, it can be shown that the same is valid for the other, a common result from ordinary quantum mechanics [38].

In the system considered, the Hamiltonian H is a 16×16 matrix. Therefore the conditions above apply for each of its elements H_{ij}. This can be easily seen by writing the Schrödinger Equation in a component-wise form:

$$\sum_{i}^{16} H_{ij} \, \Psi_i(\mathbf{r}) = \sum_{i}^{16} E \, \delta_{ij} \, \Psi_i(\mathbf{r}) \ , \tag{3.6}$$

And due to the distributive properties of commutators, it is sufficient to verify whether the condition

$$[\mathbf{L}^2, H_{ij}] = 0 \tag{3.7}$$

holds for every i, j.

In the most general case, H_{ij} has a mass term $m_{ij} \in \{2m_B, m_B + m_{B^*}, 2m_{B^*}, 0\}$, a kinetic term $T_{ij} = \frac{1}{2\mu}\left(\frac{\partial^2}{\partial r^2} + \frac{2}{r}\frac{\partial}{\partial r} + \frac{\mathbf{L}^2}{r^2}\right)\delta_{ij}$ and the interaction term, H_{int} depending on certain linear combination of radial potentials. Altogether this is

$$H_{ij} = m_{ij} + T_{ij} + H_{\text{int},ij} \ , \tag{3.8}$$

and applying the distributive property, its commutator reads

$$[\mathbf{L}^2, H_{\text{int},ij}] = [\mathbf{L}^2, m_{i,j}] + [\mathbf{L}^2, T_{ij}] + [\mathbf{L}^2, H_{\text{int},ij}] \ . \tag{3.9}$$

The commutators of the constant mass terms are null, trivially. The commutators of the non-null kinetic term are

$$\left[\mathbf{L}^2, \frac{1}{2\mu}\left(\frac{\partial^2}{\partial r^2} + \frac{2}{r}\frac{\partial}{\partial r} + \frac{\mathbf{L}^2}{r^2}\right)\right] = 0 \ , \tag{3.10}$$

which can be easily observed by expressing the operator $\mathbf{L}$ in the spatial representation

$$\mathbf{L}^2 = -\left(\frac{1}{\sin(\theta)}\frac{\partial}{\partial\theta}\left(\sin(\theta)\frac{\partial}{\partial\theta}\right) + \frac{1}{\sin^2(\theta)}\frac{\partial^2}{\partial\phi^2}\right) \tag{3.11}$$

and noting that the order of the partial derivatives is irrelevant.

Finally, the potential terms $V_5(r)$, $V_j(r)$ are spherical symmetric, implying that their superposition, given by $H_{\text{int},ij} = (\mathbb{C}^{-1})_{ik}(V)_{kl}(r)(\mathbb{C}_{lj})$, must also be, *i.e.*

$$H_{\text{int},ij} = H_{\text{int},ij}(r) \ . \tag{3.12}$$

Using an arbitrary test function $\psi(r,\Omega)$ and the $\mathbf{L}^2$ representation (3.11), it is straightforward to see that, for any arbitrary spherical symmetric function $F(r)$, the following holds

$$\mathbf{L}^2 \ (F(r)\psi(r,\Omega)) = F(r) \ \left(\mathbf{L}^2\psi(r,\Omega)\right) \tag{3.13}$$

$$\implies [\mathbf{L}^2, F(r)] = 0 \ , \tag{3.14}$$

. Thus,

$$[\mathbf{L}^2, H_{\text{int},ij}(r)] = 0 \tag{3.15}$$

and, consequently,

$$[\mathbf{L}^2, H_{ij}] = 0 \tag{3.16}$$

for every i, j. Therefore relative orbital angular momentum conserves and the system has associated quantum numbers L and L_z. This is merely a manifestation of the Noether's theorem, due to the spherical symmetry present in the relative coordinates.

It is important to remark that this is only valid for arbitrary L in this model because there are no spin-orbit terms in the Schrödinger equation, *i.e.* all the heavy spin corrections are added asymptotically to the Hamiltonian via the B/B^* masses. A more complete approach would require the computation of hyperfine lattice QCD potentials which are, in general, not spherical symmetric. They were not available for this study. Therefore, what has been done here is based only the two interacting B/B^* meson picture at large separations, which validates that in this regime the heavy spin effects are manifested in the mass difference $m_{B^*} - m_B$.

3.2 Decoupling the Schrödinger equation

Symmetry arguments will be used here, in order to simplify the coupled-channel Schrödinger Equation. First, it is of interest the characterisation of the tetraquark candidates in terms of total quantum numbers

$I(J^P)$: Isospin, total angular momentum of the state and parity

Additionally, total angular momentum $\mathbf{J}$ is given by

$$\mathbf{J} = \mathbf{L} + \mathbf{S} \ . \tag{3.17}$$

Since the relative orbital angular momentum $\mathbf{L}$ has been shown to conserve (3.16), it follows from (3.17) that total spin $\mathbf{S}$ must also conserve. Thus, the system should have the additional associated quantum numbers S, L, S_z, L_z

Note, however, that the wave function components in equation (3.3) are not organised in terms of a total spin S state. Therefore, a determined L eigenstate of equation (3.3) would be a superposition of J eigenstates. This can be circumvent by reorganising the wave functions in such a way that they label a determined S combinations of B/B^*. Formally, this is equivalent to finding a basis transformation that decomposes the spin SU(2) tensor product of 2 anti-quarks and 2 quarks, letting their irreducible

representation explicit. Such decomposition can be written as

$$\mathbf{2}\otimes\mathbf{2}\otimes\mathbf{2}\otimes\mathbf{2} = (\mathbf{3}\oplus\mathbf{1})\otimes(\mathbf{3}\oplus\mathbf{1}) \tag{3.18}$$

$$= (\mathbf{3}\otimes\mathbf{3})\oplus(\mathbf{3}\otimes\mathbf{1})\oplus(\mathbf{3}\otimes\mathbf{1})\oplus(\mathbf{1}\otimes\mathbf{1}) \tag{3.19}$$

$$= \mathbf{5}\oplus\mathbf{3}\oplus\mathbf{1}\oplus\mathbf{3}\oplus\mathbf{3}\oplus\mathbf{1}\ . \tag{3.20}$$

Although spinors are not explicitly described in this non-relativistic quantum mechanical model, the interaction term, $H_{\rm int}$, by construction, has its terms combined to reflect the spin of the pair combinations of B and B^*, *i.e.* the spin products of equation (3.19). For this reason, one can apply a basis transformation matrix C, so that CHC^{-1} gives its irreducible representation, related to (3.20). Such matrix C, then, must contain the appropriate Clebsh-Gordan coefficients that makes the decomposition $(\mathbf{3}\oplus\mathbf{1})\otimes(\mathbf{3}\oplus\mathbf{1}) = \mathbf{5}\oplus\mathbf{3}\oplus\mathbf{1}\oplus\mathbf{3}\oplus\mathbf{3}\oplus\mathbf{1}$ explicit and can be easily obtained with the help of computer algebra systems, such as *Mathematica*.

An equivalent strategy has been already used for the special case where $L = 0$ [37]. In fact, after being shown here that L and S conserve separately, the same results obtained in the $L = 0$ applies here.

The resulting $CHC^{-1}(C\Psi) = E(C\Psi)$ Schrödinger equation calculated firstly in [37] and reproduced in this study, has the following block diagonal structure

$$\left[\begin{pmatrix} \tilde{H}_{2\times2,S=0} & & & \\ & \mathbb{1}_{3\times3}\otimes\tilde{H}_{S=1,1\times1} & & \\ & & \mathbb{1}_{3\times3}\otimes\tilde{H}_{S=1,2\times2} & \\ & & & \mathbb{1}_{5\times5}\otimes\tilde{H}_{S=2} \end{pmatrix} - E\right]\begin{pmatrix} \Psi_{2\times2\ S=0} \\ \Psi_{3\times3\ S=1} \\ \Psi_{6\times6\ S=1} \\ \Psi_{5\times5\ S=2} \end{pmatrix} = 0\ , \tag{3.21}$$

i.e. the equation decouples in four blocks of independent degenerate equations in according to S:

Block 1: $S = 0$

Corresponds to a single 2×2 coupled channel equation

$$\left[\begin{pmatrix} 2m_B & \\ & 2m_{B^*} \end{pmatrix} - \frac{1}{2\mu}\boldsymbol{\nabla}^2\mathbb{1}_{2\times2} + \tilde{H}_{{\rm int},S=0}\right]\Psi_{S=0}(\mathbf{r}) = E\Psi_{S=0}(\mathbf{r}) \tag{3.22}$$

where

$$\tilde{H}_{{\rm int},S=0} = \frac{1}{4}\begin{pmatrix} V_5(r)+3V_j(r) & \sqrt{3}(V_5(r)-V_j(r)) \\ \sqrt{3}(V_5(r)-V_j(r)) & 3V_5(r)+V_j(r) \end{pmatrix} \tag{3.23}$$

and with the definition $\mathbf{B}^{*2} = B_x^*B_x^* + B_y^*B_y^* + B_z^*B_z^*$, the wave function $\Psi_{S=0}$ relates to the old wave function by:

$$\Psi_{S=0} = \begin{pmatrix} BB \\ \frac{1}{\sqrt{3}}\mathbf{B}^{*2} \end{pmatrix} \tag{3.24}$$

Block 2: $S = 1$ and symmetric under B/B^* meson exchange

There are three identical single channel equations due to the three-fold symmetry of $S = 1$, *i.e.* $j = S_z = -1, 0, 1$

$$\left[m_B + m_{B^*} - \frac{1}{2\mu}\boldsymbol{\nabla}^2 + \tilde{H}_{\text{int}S=1,1\times1}\right]\Psi_{S=1,1\times1,j}(\mathbf{r}) = E\Psi_{S=1,1\times1,j}(\mathbf{r}) \tag{3.25}$$

where

$$\tilde{H}_{\text{int},S=1,1\times1} = V_j(r) \tag{3.26}$$

$$\Psi_{S=1,1\times1,j} = \frac{1}{\sqrt{2}}\left(B_j^* B + B B_j^*\right) \tag{3.27}$$

Block 3: $S = 1$ and antisymmetric under B/B^* meson exchange

There is also a three-fold degeneracy, $j = S_z = -1, 0, 1$, but, for this case, a 2×2 coupled channel equation was obtained

$$\left[\begin{pmatrix} m_B + m_{B^*} & \\ & 2m_{B^*} \end{pmatrix} - \frac{1}{2\mu}\boldsymbol{\nabla}^2 \mathbb{1}_{2\times2} + \tilde{H}_{\text{int},S=1,2\times2}\right]\Psi_{S=1,2\times2,j}(\mathbf{r}) = E\Psi_{S=1,2\times2,j}(\mathbf{r}) \tag{3.28}$$

where

$$\tilde{H}_{\text{int},S=1,2\times2} = \frac{1}{2}\begin{pmatrix} V_5(r) + V_j(r) & V_j(r) - V_5(r) \\ V_j(r) - V_5(r) & V_5(r) + V_j(r) \end{pmatrix} \tag{3.29}$$

$$\Psi_{S=1,2\times2,j} = \frac{1}{\sqrt{2}}\begin{pmatrix} B_j^* B - B B_j^* \\ \epsilon_{jkl} B_k^* B_l^* \end{pmatrix} \tag{3.30}$$

Block 4: $S = 2$

They are five-fold degenerate ($S_z = -2, 1, 0, 1, 2$) single channel equations

$$\left[2m_{B^*} - \frac{1}{2\mu}\boldsymbol{\nabla}^2 + \tilde{H}_{\text{int},S=2}\right]\Psi_{S_z}(\mathbf{r}) = E\Psi_{S_z}(\mathbf{r}) \tag{3.31}$$

where

$$\tilde{H}_{\text{int}1,S=2} = V_j(r) \tag{3.32}$$

$$\Psi_{S=2,S_z} = 2\sqrt{\frac{2\pi}{15}} Y_2^{S_z}\left(B_x^*, B_y^*, B_z^*\right) \tag{3.33}$$

and Y^{S_z} is an abbreviation in terms of the spherical harmonic functions.

3.2.1 Symmetry of the wave functions and total quantum numbers

The simpler equations derived above are not the whole picture for a general description including arbitrary excited L states. Observe that the potentials were not yet specified with respect to light quark flavour *i.e.* the isosinglet ($I = 0$) and isotriplet ($I = 1$). As we shall see, specific choices of both I and L, changes the physical interpretation of those equations.

This becomes clear when we consider the symmetry of the $\bar{b}\bar{b}$ wave function. The fermion nature of $\bar{b}$ quarks, and therefore of $\bar{b}\bar{b}$, implies that their wave function must be antisymmetric under particle exchange. Quantum mechanically, this is equivalent to the Pauli exclusion principle. Since $\bar{b}\bar{b}$ wave functions are symmetric in the flavour space, but can be spatially symmetric, if L is even, or asymmetric, if L is odd , only particular combinations resulting in a antisymmetric total wave function are allowed. In practice, one has to consider all the symmetries (antisymmetries) related to the system's quantum numbers, in according to

$$|\Psi\rangle = |\psi_{\text{spatial}}\rangle \otimes |\psi_{\text{colour}}\rangle \otimes |\psi_{\text{flavour}}\rangle \otimes |\psi_{\text{spin}}\rangle \tag{3.34}$$

For example, consider the spatially symmetric even angular momentum state $L \in \{0, 2, \cdots\}$ for $\bar{b}\bar{b}$. With respect to the colour space, the decomposition $\bar{\mathbf{3}} \otimes \bar{\mathbf{3}} = \bar{\mathbf{6}} \oplus \mathbf{3}$ of SU(3) representations gives either antisymmetric $\mathbf{3}$ or symmetric $\bar{\mathbf{6}}$ states. $\bar{b}\bar{b}$ states, having only one flavour, are always symmetric in flavour space. Therefore, $\mathbf{3}$ states requires symmetric wave function in the spin space (spin 1) in order to have a total antisymmetric wave function. The same argument applied vice versa, requires that the $\bar{\mathbf{6}}$ states, symmetric, should have spin 0, antisymmetric.

The same logic applies for the light qq quarks with the addition that there are two flavour possibilities. Thus, the isosinglet $I = 0$, which is antisymmetric in flavour space, implies $\bar{\mathbf{3}}$ colour states having spin 0 and the symmetric $\mathbf{6}$ states having spin 1. For $I = 1$, it is the other way around and hence, the spin of the $\bar{\mathbf{3}}$ and $\mathbf{6}$ states are exchanged. Next, one can combine qq with $\bar{b}\bar{b}$ so that the resulting states are colour neutral $qq\bar{b}\bar{b}$ states. All possible combinations are shown in Table 3.1. Finally, following the same logic for for $L \in \{1, 2, \cdots\}$ determines all the possible combinations summarised in Tables 3.2.

Labelling the heavy spin by $s_{\bar{b}\bar{b}}$ and the light spin by s_{qq} the total spin S possibilities for each the each combination is given by

$$|s_{\bar{b}\bar{b}} - s_{qq}| \leq S \leq s_{\bar{b}\bar{b}} + s_{qq} \ . \tag{3.35}$$

Then total angular momentum J, given by

$$|S - L| \leq J \leq S + L \tag{3.36}$$

Finally, parity P is obtaining by firstly consider that, both B and B^*, have intrinsic (-1) parity. Therefore the $qq\bar{b}\bar{b}$ states, which can be described in term of the meson pair quantum numbers, must have intrinsic $(-1) \cdot (-1) = (+1)$ parity. The next contribution comes from the orbital angular momentum, in according to the eigenvalue relation of the spherical harmonic

$$PY_L^{L_z}(\Omega) = (-1)^L Y_L^{L_z}(\Omega) \ . \tag{3.37}$$

These considerations result in the total parity

$$P = (+1) \cdot (-1)^L = (-1)^L \tag{3.38}$$

Notice that the combinations in Tables 3.1 and 3.2 can be assigned to the different blocks of Schrödinger Equation. For doing so, one must find their respective B/B^* contents, which can be easily calculated using the Fierz identity (2.16). For example, combinations 1 and 2 are superposition of a state 1, having $s_{qq} = 0$ and $s_{\bar{b}\bar{b}} = 1$ and a state 2, having $s_{qq} = 1$ and $s_{\bar{b}\bar{b}} = 0$. The associated spin couplings are $\mathbb{L} = (\mathbb{1} + \gamma_0)\gamma_5$ and $\mathbb{S} = (\mathbb{1} + \gamma_0)\gamma_j$ for state 1, and $\mathbb{L} = (\mathbb{1} + \gamma_0)\gamma_j$ and $\mathbb{S} = (\mathbb{1} + \gamma_0)\gamma_5$ for state

	light quarks qq			heavy quarks $\bar{b}\bar{b}$			$qq\bar{b}\bar{b}$	
combination	isospin	spin	colour	spin	colour	L	S	J^P
1	0(A)	0 (A)	$\bar{3}$ (A)	1 (S)	3 (A)	$0, 2, \cdots$ (S)	1	$\lvert 1-L\rvert^+ \leq J^+ \leq \lvert 1+L\rvert^+$
2		1 (S)	6 (S)	0 (A)	$\bar{6}$ (S)			
3	1(S)	0 (A)	6 (S)	0 (A)	$\bar{6}$ (S)	$0, 2, \cdots$ (S)	0	L^+
4		1 (S)	$\bar{3}$ (A)	1 (S)	3 (A)		0, 1, 2	$\lvert S-L\rvert^+ \leq J^+ \leq \lvert S+L\rvert^+$

TABLE 3.1: Possible combinations of $qq\bar{b}\bar{b}$ quantum numbers with even L.

	light quarks qq			heavy quarks $\bar{b}\bar{b}$			$qq\bar{b}\bar{b}$	
combination	isospin	spin	colour	spin	colour	L	S	J^P
1	1(S)	0 (A)	6 (S)	1 (S)	$\bar{6}$ (S)	$1, 3, \cdots$ (A)	1	$\lvert 1-L\rvert^- \leq J^- \leq \lvert 1+L\rvert^-$
2		1 (S)	$\bar{3}$ (A)	0 (A)	3 (A)			
3	0(A)	0 (A)	$\bar{3}$ (A)	0 (A)	3 (A)	$1, 3, \cdots$ (A)	0	L^-
4		1 (S)	6 (S)	1 (S)	$\bar{6}$ (S)		0, 1, 2	$\lvert S-L\rvert^- \leq J^- \leq \lvert S+L\rvert^-$

TABLE 3.2: Possible combinations of $qq\bar{b}\bar{b}$ quantum numbers with odd L.

two. With that information, one can use the coefficients (2.17) to work out the corresponding meson contents of the superposition. This in fact, corresponds to the wave function of Block 3. Doing the same for the remaining combinations, Block 1 is determined as being combination 3 coupled to the spin 0 channel of combination 4; Block 2 is purely the spin 1 channel of combination 4; and, finally, Block 4 is the spin 2 channel of combination 4. A rapid confirmation can be performed by counting all the spin degrees of freedom of the respective combinations and seeing the agreement with the degrees of freedom of each block.

These findings are summarised in Tables 3.3 and 3.4. They show that the parity of L (even/odd) determines the quantum numbers I and P for which a certain block has a physical meaning. Namely, when the parity of L changes, the quantum numbers I and P are interchanged ($I = 0 \leftrightarrow 1$ *and* $P = (+1) \leftrightarrow (-1)$) between the blocks .

	$L = 0, 2, 4, \cdots$		
Block	S	I	J^P
1	0	1	L^+
2	1	1	$\lvert 1-L\rvert^+ \leq J^+ \leq \lvert 1+L\rvert^+$
3	1	0	
4	2	1	$\lvert 2-L\rvert^+ \leq J^+ \leq \lvert 2+L\rvert^+$

TABLE 3.3: $ud\bar{b}\bar{b}$ states, even L.

3.3 Angular momenta eingenfunctions $\mathbf{Z}_{n,L,L_z}(\Omega)$

Bound state and resonance analysis require finding the Schrödinger equation in terms of the radial coordinate r. For doing so, a description of the additional coordinates

	$L = 1, 3, 5 \cdots$		
Block	S	I	J^P
1	0	0	L^-
2	1	0	$\lvert 1-L\rvert^- \leq J^- \leq \lvert 1+L\rvert^-$
3	1	1	
4	2	0	$\lvert 2-L\rvert^- \leq J^- \leq \lvert 2+L\rvert^-$

TABLE 3.4: $ud\bar{b}\bar{b}$ states, odd L

Ω is necessary. Typically, it is achieved in a single-channel Schrödinger equation via a partial waves expansions in term of the spherical harmonics $Y_{L,L_z}(\Omega)$, *i.e.* the eigenfunctions of L and L_z

In a system of N coupled Schrödinger equations, one needs a more general approach. This is a problem found typically in molecular chemical physics [39–41]. In this study, we base in a similar approach presented in [42]. Giving a set of observable $\tilde{L}, \tilde{L}_z$ that are conserved under Ω transformation, one needs to find a set of N-dimensional eigenfunctions $\mathbf{Z}_{n,\tilde{L},\tilde{L_z}}(\Omega)$, forming a basis for the space of $\Psi(r,\Omega)$. Such set needs to be complete and orthogonal with respect to the solid angle Ω and to N, so that the n-component of wave function can be decomposed

$$\psi_n(r,\Omega) = \sum_{L}^{\infty} \sum_{L_z=-L}^{L} R_{L,L_z}(r) \cdot \mathbf{Z}_{n,L,L_z}(\Omega) \ , \tag{3.39}$$

where

$$R_{L,L_z}(r) \equiv \begin{pmatrix} R_{1,L,L_z}(r) \\ \vdots \\ R_{N,L,L_z}(r) \end{pmatrix} \ , \tag{3.40}$$

or in terms of the total wave function,

$$\Psi(r,\Omega) = \sum_{n}^{N} \sum_{L}^{\infty} \sum_{L_z=-L}^{L} R_{n,L,L_z}(r) \mathbf{Z}_{n,L,L_z}(\Omega) \ . \tag{3.41}$$

In our system $N = 16$ is the total number of channels. Therefore ψ_n is the wave function of the n-th B/B^* pair channel ($\psi_n \in \{BB, BB_x^*, \cdots, B_z^* B_z^*\}$). Because L conserves, the spherical harmonics $Y_{L,L_z}(\Omega)$ form a common set of basis for each n-th wave function[2]. Therefore, eigenfunctions satisfying the completeness and orthonormality conditions can be constructed to be column vectors $\mathbf{Z}_{n,L,L_z}(\Omega)$ having spherical harmonics in the n-th column as the only non-zero element *i.e.*

$$\left[\mathbf{Z}_{n,L,L_z}(\Omega)\right]_{n'} = Y_{L,L_z}(\Omega)\delta_{n,n'} \quad \text{for } n \in 1, 2, \cdots 16 \tag{3.42}$$

[2]Note that this is also true for the $S \neq 0$ channels. There are no S-L couplings in the approach used of adding $\bar{b}\bar{b}$ asymptotically and, consequently, L was shown to conserve.

In fact, their orthornormality relation will follow from the orthornormality of the spherical harmonics

$$\int \mathrm{d}\Omega\ \mathbf{Z}^{\dagger}_{n,L,L_z}(\Omega)\mathbf{Z}_{n',L',L'_z}(\Omega) = \delta_{n,n'} \int \mathrm{d}\Omega\ Y^{*}_{L,L_z}(\Omega)Y_{L',L'_z}(\Omega) \tag{3.43}$$

$$= \delta_{n'_n}\delta_{L,L'}\delta_{L_z,L'_z}\ . \tag{3.44}$$

And from that one can easily verify that they satisfy a completeness relation

$$\sum_{n}^{N}\sum_{L}^{\infty}\sum_{L_z=-L}^{L} \mathbf{Z}_{n,L,L_z}(\Omega')\mathbf{Z}^{\dagger}_{n,L,L_z}(\Omega) = \sum_{L}^{\infty}\sum_{L_z=-L}^{L} \left(Y^{*}_{L,L_z}(\Omega)Y_{L,L_z}(\Omega')\right)\ \mathbb{1}_{N\times N} \tag{3.45}$$

$$= \frac{\delta(\Omega-\Omega')}{\sin\theta}\ \mathbb{1}_{N\times N}. \tag{3.46}$$

In the system considered, there are a total of $16 \times L \times (2L+1)$ eigenfunctions $\mathbf{Z}_{n,L,L_z}(\Omega)$, having each 16-components. Nevertheless, due to the decoupling of the system in smaller dimensional equation, *i.e.* there is a block diagonal representation, it is sufficient to analyse each independent block of equation separately, without loss of generality. Considering that, the 2×2 blocks have each $2\times L\times(2L+1)$ eigenfunction given by:

$$\mathbf{Z}_{1,L,L_z}(\Omega) = (Y_{L,L_z}(\Omega), 0)\ , \tag{3.47}$$

$$\mathbf{Z}_{2,L,L_z}(\Omega) = (0, Y_{L,L_z}(\Omega))\ , \tag{3.48}$$

while the 1×1 independent equations have $L\times(2L+1)$ eigenfunctions, which are simply the spherical harmonics themselves,

$$Z_{L,L_z}(\Omega) = Y_{L,L_z}(\Omega)\ . \tag{3.49}$$

Chapter 4

Bound states for excited L states

In the last chapter, a formalism was set allowing the connection between the Schrödinger equations and the total quantum numbers, for an arbitrary L. Additionally, generalised angular eigenfunctions for the couple channel equation, $\mathbf{Z}_{L,L_z}(\Omega)$, were described. In this chapter, we proceed to the investigation of tetraquark states by means of a bound states analysis. The interesting channel has quantum numbers $I(J^P) = 0(1^-)$. There are a total of four possibilities in Table (3.4) providing these total quantum number. They are

- Block 1 with $L = 1$:

$$\text{Coupled-channel of } BB \text{ and } B^*B^* \text{ with } S = 0;$$

- Block 2, with $L = 1$:

$$\text{Single } \tfrac{1}{\sqrt{2}}(BB^* + B^*B) \text{ channels with } S = 1;$$

- Block 3, with $L = 1$ and $L = 3$:

$$\text{Single } B^*B^* \text{ channels with } S = 2.$$

Blocks 2 and 3, given by (3.25) and (3.31), have only potential terms proportional to $V_j(r)$. This is a repulsive potential for isospin $I = 0$, as a result of the light and the heavy quarks being in an repulsive colour sextet, 6 and $\bar{6}$, as previously shown (Table 3.2). Those cannot form bound states and are, hence, excluded. Therefore, Block 1, having combinations of the attractive V_5 and the repulsive V_j is the only remaining candidate that could possibly host a tetraquark.

Previous studies, even without accounting for heavy spin effects have found no bound states with quantum numbers $I(J^P) = 0(1^-)$ [29, 32]. Adding heavy spin-effects would not change this picture because they are expected to lower the binding energy of the states. There is, thus, no expectation in finding physical bound states at this channel, nonetheless a bound state study for heavier masses can provide new insights.

4.1 The radial equation for S = 0

A partial waves expansion is performed by using the generalised eigenfunctions $\mathbf{Z}_{L,L_z}(\Omega)$. For the $S = 0$ (2×2) the expanded wave function is

$$\Psi(\mathbf{r})_{S=0} = \sum_{n=1,2} \sum_{L}^{\infty} \sum_{L_z=-L}^{L} \frac{u_{n,L,L_z}(r)}{r} \mathbf{Z}_{n,L,L_z}(\Omega) \ , \tag{4.1}$$

with eigenfunctions given by (3.47) and (3.48). Substituting the expansion in equation (3.22) and using the orthogonality relations (3.44) allow the determination of the radial equation by performing the following projections

- $\int \mathrm{d}\Omega\ (\mathbf{Z}_{1,L,L_z}(\Omega))^\dagger (H_{S=0} - E)\Psi_{S=0} = 0$:

$$\left[2m_B + \frac{P_L^2}{2\mu} + \frac{V_5 + 3V_j}{4} - E\right] u_{1,L,L_z}/r + \left[\frac{\sqrt{3}(V_5 - V_j)}{4}\right] u_{2,L,L_z}/r = 0\ , \quad (4.2)$$

- $\int \mathrm{d}\Omega\ (\mathbf{Z}_{2,L,L_z}(\Omega))^\dagger (H_{S=0} - E)\Psi_{S=0} = 0$:

$$\left[2m_{B^*} + \frac{P_L^2}{2\mu} + \frac{3V_5 + V_j}{4} - E\right] u_{2,L,L_z}/r + \left[\frac{\sqrt{3}(V_5 - V_j)}{4}\right] u_{1,L,L_z}/r = 0\ , \quad (4.3)$$

where

$$P_L^2 = -\left(\frac{\partial^2}{\partial r^2} + \frac{2}{r}\frac{\partial}{\partial r} - \frac{L(L+1)}{r^2}\right)\ . \quad (4.4)$$

These two equations can be summarised in a matrix form:

$$\left[\begin{pmatrix} 2m_B & \\ & 2m_{B^*} \end{pmatrix} + \frac{P_L^2}{2\mu} + \tilde{H}_{\mathrm{int},S=0}(r)\right] \mathbf{u}_L(r)/r = E\mathbf{u}_L(r)/r\ , \quad (4.5)$$

with

$$\mathbf{u}_L(r) = \begin{pmatrix} u_{1,L}(r) \\ u_{2,L}(r) \end{pmatrix}\ . \quad (4.6)$$

Observe that the interaction term $\tilde{H}_{\mathrm{int},S=0}$ for the radial equations with definite L is exactly the same as the one for the full stationary Schrödinger equation (3.23). Therefore, no further couplings are added into the system when compared to the $L = 0$ case. Also, note that the subscript L_z was removed in the wave function. That is motivated by the fact for a spherical symmetric potential ($M + H_{\mathrm{int}}(r)$) the solutions are degenerate with respect to L_z, *i.e.* the total wave functions have cylindrical symmetry.

By multiplying both sides of the equation by r, the partial differential equation can be reduced to an ordinary one. The resulting equation, after subtracting out the upper limit threshold for bound states $2m_B$, becomes

$$\left[\begin{pmatrix} 0 & \\ & 2\Delta m_S \end{pmatrix} - \frac{1}{2\mu}\left(\frac{\mathrm{d}^2}{\mathrm{d}r^2} - \frac{L(L+1)}{r^2}\right) + \tilde{H}_{\mathrm{int,S=0}}(r)\right] \mathbf{u}_L(r) = -\Delta E \mathbf{u}_L(r)\ , \quad (4.7)$$

where a renaming of variables was performed, in order to define the spin splitting term

$$\Delta m_S \equiv m_{B^*} - m_B\ , \quad (4.8)$$

and the binding energy

$$\Delta E \equiv m_B - E\ . \quad (4.9)$$

Given an attractive potential, it is well-known that bound states are present if the constituent particles are heavy enough. Hence, we aim at increasing the kinetic mass $\mu = m_b/2$ to nonphysically heavy values, finding the threshold for which bound

state appears. Naturally, increasing the masses of the bare $\bar{b}$ antiquarks will cause an effect in the masses of the pseudoscalar B and vector B^* meson and, consequently, in the Δm_S term. In order to address that, we rely on results from Heavy Quark Effective Field Theory ($HQEFT$) relating the mass of a heavy quark to the mass of its corresponding heavy-light mesons, such as B's and D's [43, 44]. Particularly, it states that the mass m_j of the meson (here $j = B, B^*$) is given, to order $1/m_b$, by the expansion[45]

$$m_j = m_b + \bar{\Lambda} + \frac{\mu_\pi^2}{2m_b} - d_j \frac{\mu_G^2}{2m_b} + \mathcal{O}(1/m_b^2) \ , \tag{4.10}$$

where has $d_B = 3$ for the spin-0 B-meson and $d_{B^*} = -1/3$ for the spin-1 B^*-meson. In the relation above $\bar{\Lambda}$ is the energy of the constituent light quarks and gluons, $\mu_\pi^2/2m$ is the heavy quark's kinetic energy, and $\mu_G^2/2m$ is the spin-orbit interaction term. Note that the only term varying between the masses of B and B^* is the spin-orbit interaction, which is proportional to $1/m_b$. Equation (4.10), thus, implies that

$$m_{B^*} - m_B \propto 1/m_b \ . \tag{4.11}$$

Consequently, when m_b is increased by a factor κ, the respective new mass and spin splitting term entering equation (4.7) are

$$m_b' = \kappa m_b \ , \tag{4.12}$$

$$\Delta {m_S}' = \frac{\Delta m_S}{\kappa} \ . \tag{4.13}$$

Observe that (4.13) implies that for $k \to \infty$, namely infinitely heavy and, thus, static b quarks/anti-quarks, the spin splitting vanishes, agreeing with the static approximation where B and B^* mesons are degenerate.

4.2 Numerical Solution

Equation (4.7) can be solved numerically by generalising the well-known quantum mechanical boundary conditions for bound states [38] to a 2×2 coupled Schrödinger Equation

$$\lim_{r \to 0} \mathbf{u}_L(r) = \begin{pmatrix} 0 \\ 0 \end{pmatrix}, \tag{4.14}$$

$$\lim_{r \to \infty} \mathbf{u}_L(r) = \begin{pmatrix} 0 \\ 0 \end{pmatrix} \ . \tag{4.15}$$

Numerically, both of these conditions are problematic. Firstly, the potentials V_5 and V_j are singular at $r = 0$. That leads to numerical instabilities, making (4.14) impracticable. Secondly, $r = \infty$ is a mathematical concept that cannot be defined numerically. The first is addressed by finding corresponding boundary conditions for a small, but finite, $r = \epsilon$. Giving that V_5 and V_j diverge slower than $1/r^2$ for $r \to 0$, the centrifugal term dominates in equation (4.7) at $r = \epsilon$. Thus the equation is approximate by a free Schrödinger Equation

$$\left[\begin{pmatrix} 0 & \\ & 2\Delta m_B \end{pmatrix} - \frac{1}{2\mu} \left(\frac{\mathrm{d}^2}{\mathrm{d}r^2} - \frac{L(L+1)}{r^2} \right) \right] \mathbf{u}_L(r) = -\Delta E \mathbf{u}_L(r) \ . \tag{4.16}$$

Generalising knowing concepts from one-dimensional quantum mechanics, the equation can be solved by the anzätze $\mathbf{u}_L(r) \sim (A, B)r^{L+1}$ and $\mathbf{u}_L(r) \sim (C, D)r^{-L}$. The wave function must be regular at the origin (4.14), that means that only solutions of the type $\sim r^{L+1}$ are accepted. That motivates the following boundary conditions:

$$\mathbf{u}_L(r) \sim \begin{pmatrix} A_1 \\ A_2 \end{pmatrix} r^{L+1} \quad \text{for } r \to 0 \ . \tag{4.17}$$

They also guarantee that the correct asymptotic behaviour given of the derivative holds, *i.e.*

$$\frac{\mathrm{d}\mathbf{u}_L(r)}{\mathrm{d}r} \sim \begin{pmatrix} A_1 \\ A_2 \end{pmatrix} (L+1)r^{L} \quad \text{for } r \to 0 \ . \tag{4.18}$$

The second problem is addressed by noting that the potentials V_5 and V_j are short-ranged. The normalisation condition of the wave function (4.15) can than be loosened to require only that they must vanish at $r = r_{\max}$, provided $r_{\max}$ is large enough to be far outside of the range of the potentials. That means

$$\mathbf{u}_L(r_{\max}) = \begin{pmatrix} 0 \\ 0 \end{pmatrix} \ . \tag{4.19}$$

Finding a bound state corresponds to determine the independent variables A_1, A_2 and ΔE for which these boundary conditions are satisfied. This boundary value problem can be solved by using different well established numeric routines One example is the combination of the shooting method with a two-dimensional root-finding algorithm [46] In this study, we avoid the multi-dimensional root finding problem by doing further developments appropriated for 2×2 case, where the boundary value problem is reduced to a one-dimensional root-finding problem for the variable ΔE.

Consider two different solutions $\mathbf{u}_L^{(1)}(r)$ and $\mathbf{u}_L^{(2)}(r)$ of equation (4.7) which are defined to have the following the asymptotic behaviour

$$\mathbf{u}_L^{(1)}(r) = \begin{pmatrix} 1 \\ 0 \end{pmatrix} r^{L+1} \quad \text{for} \ \ r \to 0 \ , \tag{4.20}$$

$$\mathbf{u}_L^{(2)}(r) = \begin{pmatrix} 0 \\ 1 \end{pmatrix} r^{L+1} \quad \text{for} \ \ r \to 0 \ , \tag{4.21}$$

fulfilling (4.17) and (4.18). Because equation (4.7) is linear, a linear combination of these two solutions builds a more general solution $\mathbf{u}_L = A_1\mathbf{u}_L^{(1)} + A_2\mathbf{u}_L^{(2)}$, which can be enforced to fulfil (4.19). Therefore for $r = r_{\max}$ outside the range of the potential, (4.19) is modified to

$$\mathbf{u}_L(r_{\max}) = A_1\mathbf{u}_L^{(1)}(r_{\max})) + A_2\mathbf{u}_L^{(2)}(r_{\max})) = \begin{pmatrix} 0 \\ 0 \end{pmatrix} \ , \tag{4.22}$$

which holds for appropriate A_1, A_2 and ΔE. The boundary value problem at $r_{\max}$ consists now of a linear system. The existence of non-trivial solutions for A_1 and A_2

requires that

$$\det\begin{pmatrix} u_{1,L}^{(1)}(r_{\max}) & u_{1,L}^{(2)}(r_{\max}) \\ u_{2,L}^{(1)}(r_{\max}) & u_{2,L}^{(2)}(r_{\max}) \end{pmatrix} = 0 \ . \tag{4.23}$$

This condition is independent on A_1/A_2, thus the values of ΔE for which it is satisfied can be determined via an one-dimensional root finding algorithm. Once the solutions with eigenvalue ΔE are found, A_1/A_2 can be determined via (4.22) *i.e.*

$$A_1/A_2 = -\frac{u_{1,L}^{(2)}(r_{\max})}{u_{1,L}^{(1)}(r_{\max})} = -\frac{u_{2,L}^{(2)}(r_{\max})}{u_{2,L}^{(2)}(r_{\max})} \ . \tag{4.24}$$

The numeric strategy implemented to find the eigenvalues of (4.7), when existent, is the so-called shooting method. It consisted of computing the solutions $\mathbf{u}_L^{(1)}(r)$ and $\mathbf{u}_L^{(2)}(r)$ for a certain ΔE via a 4-th order Runge Kutta [46], iterate from $r = \epsilon$ to $r_{\max}$, where the determinant of equation (4.23) is calculated. The energy ΔE for which (4.23) holds is determined by further iterations via a Newton-Rhapson root finding algorithm [46].

4.3 Results and Discussion

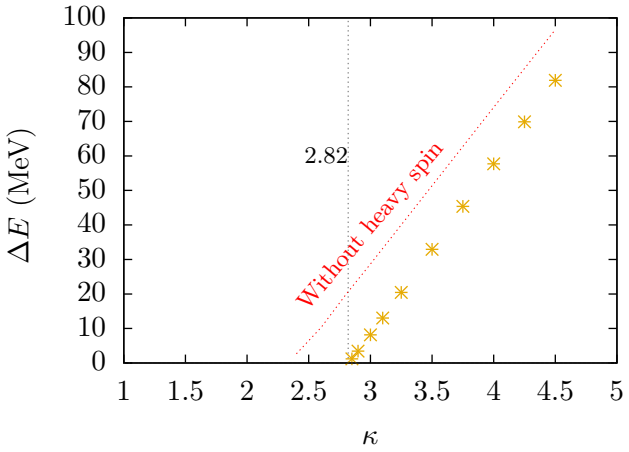

FIGURE 4.1: Bound states binding energy ΔE as a function of κ, the factor of increase in m_b. Yellow stars are bound state solution of equation (4.7) with the mean value static potentials with $I = 0$ ($\alpha_5 = 0.34$, $d_5 = 0.45$,$\alpha_j = 0.10$, $d_j = 0.28$) and dashed red lines corresponds to the approximation where heavy spin is disregarded. Here stability was guaranteed for $r_{\max} \approx 5$ fm.

Figure 4.1 is a plot of the bound state binding energy as a function of the factor κ by which the $\bar{b}$ quark masses are increased, in according to (4.12) and (4.13). Results for the simpler case where the heavy spin are not considerate, meaning that its correspondent Schrödinger Equation becomes a one-dimensional one with a single V_5 potential term, are also computed and shown for comparison. Bound states appear for κ greater than ~ 2.8 with heavy spin effects and ~ 2.3 without heavy spin. Moreover, the binding energy increases linearly with the mass in both scenarios. This suggests

that the main influence of the heavy spin in the bound states is to shift their binding energy downwards. Additionally, this shift appears to turn smaller the bigger the masses are. For $k = 2.8$, the shift is of order of ~ -20 MeV in the binding energy.

Chapter 5

Resonance search at $I(J) = 0(1^-)$

In the present chapter the Spin-0 Schrödinger Equation will be solved via a scattering theory approach. The aim is the direct search for the resonance with quantum numbers $I(J) = 0(1^-)$. This, if existent, is thought to have a mass of approximately $M = 10576^{+4}_{-4}$ MeV [32], which is above the $2m_B$ threshold, but bellow $2m_{B^*}$. Therefore it would be a resonance with respect to the BB-channel, but a bound state for the $\mathbf{B}^{*2}$-channel. Hence, scattering and bound state treatment have to be combined.

The scattering channel follows with a few adaptations to the general idea of the quantum mechanical scattering theory. It consists of expanding the wave function in terms of a particular set of eigenfunctions having the property of being conveniently matched to the scattered wave function asymptotically. A partial analysis is then used to separate the eigenfunctions' radial and angular part and to relate them with common quantities, such as scattering matrices and phase-shifts.

5.1 Theoretical foundation

5.1.1 The scattering solution

Let $\psi_k(\mathbf{r})$ be the eigenstates with energy $E = k^2/(2\mu)$ of a one-dimensional Hamiltonian with potential $v(\mathbf{r})$, satisfying the Schrödinger Equation

$$\left(\frac{\nabla^2}{2\mu} + v(\mathbf{r})\right)\psi_k(\mathbf{r}) = E_k\psi_k(\mathbf{r}) \ . \tag{5.1}$$

This equation can be also written in integral form [1]

$$\psi_k(\mathbf{r}) = N\mathrm{e}^{i\mathbf{k}\cdot\mathbf{r}} - \frac{\mu}{2\pi}\int \mathrm{d}^3r' G_+(\mathbf{r},\mathbf{r}')v(\mathbf{r}')\psi_k(\mathbf{r}') \tag{5.2}$$

where

$$G_+(\mathbf{r},\mathbf{r}') = \frac{\mathrm{e}^{i\mathbf{k}|\mathbf{r}-\mathbf{r}'|}}{\mathbf{r}-\mathbf{r}'} \tag{5.3}$$

is the retarded *Green's function*, identified as an outgoing spherical wave.

Formally, $G_+(\mathbf{r},\mathbf{r}')$ is only one of infinitely many possible *Green's function*. But, this particular choice imposes the specific boundary conditions on the eigenfunctions $\psi_k(\mathbf{r})$ which are appropriated for the description of scattering of a incoming particle (wave packet) into a potential. The convenience of this choice is best seen in the

[1] This is a well known result from textbook's quantum mechanics[38]. Formally it follows from the *Green's function*[47] method for solving inhomogeneous differential equations: Given an inhomogeneous wave equation $(\nabla^2+k^2)\psi = U\psi$, a solutions can be constructed by adding a particular solution $\frac{1}{4\pi}\int \mathrm{d}^3G(\mathbf{r},\mathbf{r}')v(\mathbf{r}'))\psi_k(\mathbf{r}')$ to the solution of its homogeneous part (plane wave), where $G(\mathbf{r},\mathbf{r}')$ is one of the infinitely many *Green's function* defined by the equation $(\nabla^2+k^2)G(\mathbf{r},\mathbf{r}') = -4\pi\delta(\mathbf{r}-\mathbf{r}')$.

asymptotically limit where, for large r, the set of stationary solutions takes the form

$$\psi_k(\mathbf{r}) \approx N\left(\mathrm{e}^{i\mathbf{k}\cdot\mathbf{r}} + f_k(\Omega)\frac{\mathrm{e}^{ikr}}{r}\right) , \tag{5.4}$$

namely, it is a sum of a plane wave and outgoing spherical wave. There

$$f_k(\Omega) = \frac{\mu}{2\pi N}\int \mathrm{d}^3r'\mathrm{e}^{i\mathbf{k}'\mathbf{r}}v(\mathbf{r}')\psi_k(\mathbf{r}') \tag{5.5}$$

is the scattering amplitude and contains all the angular dependence (Ω) of the spherical wave.

Equation (5.4), thus, illuminates the idea that the scattering problem can be treated as a sum of a incoming plane wave, or, more generally, a superposition of plane waves, that are scattered in all directions after interacting with a potential. Such potential asymptotically, is equivalent to a source of outgoing spherical waves. In fact, the determination of the probability of detection arising from a scattered wave packet constructed with these eigenfunctions provides the connection between the scattering amplitude and the differential scattering cross section, a well-know result from quantum mechanics:

$$\frac{\mathrm{d}\sigma}{\mathrm{d}\Omega} = |f_k(\Omega)|^2 \tag{5.6}$$

5.1.2 Partial waves and phase shifts

It is helpful to expand (5.4) in partial waves and compare it with the separable solutions of the central potential problem, analogous to the ones that were used in the bound state analysis (4.1):

$$\psi_{k,l} = R_{l,k}(r)Y_{l,l_z}(\Omega) = \frac{u_{l,k}}{r}Y_{l,l_z}(\Omega) \ . \tag{5.7}$$

Given a spherical symmetric potential, such the ones treated here, the scattered wave packets will have cylindrical symmetry. Hence, there is no dependence on the azimutal angle ϕ and one can choose freely the direction z as the direction of the incident wave. Therefore, only terms $Y_{l,0} \sim P_l(\cos\theta)$ appears, where $P_l(\cos\theta)$ are the Legendre Polynomials. Exploring these symmetries, the partial waves expansion is

$$\psi_k = \sum_{L=0} i^l(2l+1)R_{l,k}(r)P_l(\cos(\theta)) \ . \tag{5.8}$$

Using the same arguments one can look to the partial waves expansion of the asymptotic behaviour (5.4). The expansion of the plane wave and the scattering amplitude are, respectively

$$e^{i\boldsymbol{k}\boldsymbol{x}} = \sum_{l=0}^{\infty} i^l(2l+1)j_l(kr)P_l(\cos\theta), \tag{5.9}$$

$$f_k(\Omega) = f_k(\theta) = \sum_{l=0}^{\infty}(2l+1)\frac{t_l}{k}P_l(\cos\theta), \tag{5.10}$$

where (5.10) defines the partial waves expansion coefficient t_l/k.

Using expressions (5.9) and (5.10) together with the well-know asymptotic behaviour of the first order spherical Hankel functions, which is

$$h_l^{(1)}(kr) \sim \frac{-i\mathrm{e}^{i}(kr - l\pi/2)}{kr} \ , \tag{5.11}$$

results in a expression for the partial expansion in terms of the spherical functions

$$\psi_k(\mathbf{r}) \approx \sum_{l=0}^{\infty} i^l(2l+1)P_l(\cos\theta)\Big(j_l(kr) + it_l(k)h_l^{(1)}(kr)\Big) \quad \text{for } r \to \infty \tag{5.12}$$

Comparison of (5.8) and (5.12) hence provides the asymptotic ($r \to \infty$) boundary conditions of $R_{l,k} = u_{l,k}/r$:

$$R_{l,k}(r) \approx j_l(kr) + it_l h_l^{(1)}(kr) \quad \text{for } r \to \infty \tag{5.13}$$

5.1.3 Connection to experimental observables

In the absence of a scatter, one expects that the solution is that of a free Schrödinger equation, *i.e.* only terms $\sim j_l(kr)$ should remain at (5.13). For this reason, t_l is a quantity measuring the influence of the potential $v(r)$ in the system. In order to comprehend that better, one can express the asymptotic condition in terms of an incoming and an outgoing spherical wave

$$R_{l,k}(r) \approx \frac{1}{2}\Big(h_l^{(2)}(kr) + s_l h_l^{(1)}(kr)\Big) \quad \text{for } r \to \infty \tag{5.14}$$

where s_l is defined via

$$s_l \equiv 1 + 2it_l \tag{5.15}$$

and the relation between the spherical functions $j_l(kr) = 1/2(h_l^{(1)} + h_l^{(2)})$ was utilised. The complex coefficients s_l are the eigenvalues of the so-called scattering matrix. It is a k-dependent scattering amplitude and has the property of being unitary, namely $|s_l(k)|^2 = 1$ [2]. Hence, it must be of the form:

$$s_l(k) = \mathrm{e}^{2i\delta_l(k)} \tag{5.16}$$

defining the scattering phase shift $\delta_l(k)$.

Observe that $\delta_l(k) = 0$ implies $s_l = 1$ and $t_l = 0$ and the solution of the free system $\sim j_l(kr)$ is recovered. When, in turn, $\delta_l(k) \neq 0$ the outgoing spherical waves contains a phase-shift at large r, as a result of the presence of a scattering potential.

Finally, inserting (5.10) on (5.6) with the help of the relations (5.15) and (5.16) determines the total scattering cross in terms of the phase-shift

$$\sigma = \int \mathrm{d}\sigma \frac{\mathrm{d}\sigma}{\mathrm{d}\Omega} = \sum_{l=0}^{\infty} \frac{4\pi}{k^2}(2l+1)\sin\delta_l \ , \tag{5.17}$$

where the contributions from each partial waves are

$$\sigma_l = \frac{4\pi}{k^2}(2l+1)\sin\delta_l \ . \tag{5.18}$$

[2] Formally that is a consequence of the conservation of the probability density for each partial wave, following from the requirement that the radial current $j_r \sim (1 - |s_l(k)|^2)$ satisfies $j_r = 0$.

Since σ is a measurable quantity, this establishes the connection between theory and experiment in the scattering problem.

5.2 The coupled $S = 0$ system

These concepts can now be applied to the 2x2-coupled equations with $S = 0$. We are particularly interested in a resonance with energy $2m_B < E_{\text{res}} < 2m_{B^*}$. The emergent wave method is used, where the channel BB is written as

$$\mathbf{\Psi}_{BB}(r,\Omega) = N\mathrm{e}^{i\mathbf{k}\cdot\mathbf{r}} + X(r) \ . \tag{5.19}$$

$X(r)$ is the emergent wave, which is expected to be an outgoing spherical wave asymptotically, as the one discussed in the last section. With that, the asymptotic boundary condition for this channel for large r would be of the form of (5.4).

Since the resonance is bellow the $2m_{B^*}$ threshold, no emergent wave is expected in the $\mathbf{B}^{*2}$-channel. Therefore this channels is treated as a bound state problem. The two-dimensional wave function reads

$$\mathbf{\Psi}(\mathbf{r}) = \begin{pmatrix} N\mathrm{e}^{i\mathbf{k}\cdot\mathbf{r}} + X(\mathbf{r}) \\ \psi_{\mathbf{B}^{*2}}(\mathbf{r}) \end{pmatrix} , \tag{5.20}$$

A partial waves expansion of each term in terms of the two dimensional generalised eigenfunctions $\mathbf{Z}_{n,L,L_z}(\Omega)$ is performed, resulting in

$$N\mathrm{e}^{i\mathbf{k}\cdot\mathbf{r}} = \sum_{L,L_z} c_{L,L_z}\, j_L(kr)\, Y_{L,L_z}(\Omega) \ , \tag{5.21}$$

$$X(\mathbf{r}) = \sum_{L,L_z} c_{L,L_z}\, \frac{\chi_{L,L_z}(r)}{kr}\, Y_{L,L_z}(\Omega) \ , \tag{5.22}$$

$$\psi_{\mathbf{B}^{*2}}(\mathbf{r}) = \sum_{L,L_z} c_{L,L_z}\, \frac{u_{L,L_z}(r)}{kr}\, Y_{L,L_z}(\Omega) \ , \tag{5.23}$$

where the prefactors ${c_{L,L_z}}^3$, from the plane wave expansion (5.21), and $1/(kr)$ are included in (5.22) and (5.23) aiming at simplifying the radial Schrödinger equation. Thus the partial waves expansion of the total wave function is

$$\mathbf{\Psi}(r,\Omega) = \sum_n \sum_{L,L_z} R_{n,L,L_z}(r)\mathbf{Z}_{n,L,L_z}(\Omega) \ , \tag{5.24}$$

with

$$\mathbf{R}_{L,L_z}(r) = c_{L,L_z} \begin{pmatrix} j_L(kr) + \chi_{L,L_z}(r)/(kr) \\ u_{L,L_z}(r)/(kr) \end{pmatrix} . \tag{5.25}$$

With help of the orthornormality relations for $\mathbf{Z}_{n,L,L_z}$ (3.44) one can perform the following projections

- $\int \mathrm{d}\Omega\ (\mathbf{Z}_{1,L,L_z}(\Omega))^\dagger (H_{S=0} - E)\Psi_{S=0} = 0$:

[3] c_{L,L_z} can be determined using (5.9) to calculate the projection $\int \mathrm{d}\Omega Y^*_{L,L_z}(\Omega) N\mathrm{e}^{i\mathbf{k}\cdot\mathbf{r}} = [4\pi(2L+1)]^{1/2} i^L j_L(kr)$. That gives $c_{L,L_z} = [4\pi i^L(2L+1)]^{1/2}$.

$$\left[2m_B + \frac{P_L^2}{2\mu} + 1/4(V_5 + 3V_j) - E\right] c_{L,L_z}[j_L(kr) + \chi_{L,L_z}(r)/(kr)] + \sqrt{3}/4(V_5 - V_j)]\, c_{L,L_z} u_{L,L_z}(r)/(kr) = 0 \ , \quad (5.26)$$

- $\int \mathrm{d}\Omega\ (\mathbf{Z}_{2,L,L_z}(\Omega))^\dagger (H_{S=0} - E)\Psi_{S=0} = 0$:

$$\left[2m_{B^*} + \frac{P_L^2}{2\mu} + 1/4(3V_5 + V_j) - E\right] c_{L,L_z} u_{L,L_z}(r)/(kr) + \sqrt{3}/4(V_5 - V_j)\, c_{L,L_z}[j_L(kr) + \chi_{L,L_z}(r)/(kr)] = 0 \ , \quad (5.27)$$

or in matrix form representation, after subtracting the threshold $2m_B$ and dividing both sides by c_{L,L_z}

$$\left[\begin{pmatrix} 0 & \\ & 2\Delta m_S \end{pmatrix} + \frac{P_L^2}{2\mu} + \tilde{H}_{\mathrm{int,S=0}}(r) - E_{\mathrm{res}}\right] \begin{pmatrix} j_L(kr) + \chi_{L,L_z}(r)/(kr) \\ u_{L,L_z}(r)/(kr) \end{pmatrix} = 0 \ . \quad (5.28)$$

Using that the plane wave is the solution of the free Schrödinger equation, namely

$$\frac{P_L^2}{2\mu} j_L(kr) = E_{\mathrm{res}} j_L(kr) \ , \quad (5.29)$$

to perform further simplifications and introducing the abbreviations

$$\boldsymbol{\phi}_L(r) = \begin{pmatrix} \chi_L(r) \\ u_L(r) \end{pmatrix} \ , \ \mathbf{U}(r) = \frac{1}{4} \begin{pmatrix} V_5(r) + 3V_j(r) \\ \sqrt{3}(V_5(r) - V_j(r)) \end{pmatrix} \ , \quad (5.30)$$

$$V_{S=0,2\times 2}(r) = \mathrm{diag}(0\,,\, 2\Delta m_S) + \tilde{H}_{\mathrm{int,S=0}}(r) \ , \quad (5.31)$$

the final equation reads

$$\left[-\frac{1}{2\mu}\left(\frac{\mathrm{d}^2}{\mathrm{d}r^2} - \frac{L(L+1)}{r^2}\right) + V_{S=0,2\times 2}(r) - E_{\mathrm{res}}\right] \boldsymbol{\phi}_L(r) = -\mathbf{U}(r) kr j_L(kr) \ . \quad (5.32)$$

5.2.1 Boundary conditions

By the same arguments made in the bound state study (Section 4.2), the asymptotic values for $r \to 0$ must be

$$\chi_L(r) \sim r^{L+1} \quad \text{for} \quad r \to 0 \quad (5.33)$$

$$u_L(r) \sim r^{L+1} \quad \text{for} \quad r \to 0 \quad (5.34)$$

$$(5.35)$$

For separations much larger than the potential ranges d_x *i.e.* $r >> d_x$ $(x = 5, j)$, where the potential terms are suppressed, the asymptotic values for $\chi_L(r)$ are obtained in according to (5.13), *i.e.* the emergent wave is a superposition of spherical waves

$$\frac{\chi_L(r)}{kr} = i t_L h_L^{(1)}(kr) \ . \quad (5.36)$$

The bound state channel should vanish for large r, as previously discussed in the short bound state analysis [4]. This time, however, it is appropriate to use its asymptotic behaviour, so that the boundary condition on $\chi_L(r)$ and $u_L(r)$ can be obtained at a same $r_{\max}$. It reads

$$\frac{u_L(r)}{kr} = b_L h_L^{(1)}(iqr) \tag{5.37}$$

where b_L is a coefficient determined from the boundary conditions.

5.3 Numerical Solution

Equation (5.32) is an inhomogeneous differential equation. Theory of elementary linear differential equations states that their general solution is a sum of one particular solution with the general solution of their homogeneous equation counterpart, *i.e.* the complementary equation [48]. The complementary equation, in fact, is the equation studied in the bound states analysis, but now subject to a different boundary conditions for large r. Thus, following the same strategy as before, we iterate, via a 4-th order Runge Kutta algorithm, solutions of the homogeneous equation $\boldsymbol{\phi}_{H,L}^{(1)}(r)$ and $\boldsymbol{\phi}_{H,L}^{(2)}(r)$ that have linear independent asymptotic values at $r = \epsilon$:

$$\boldsymbol{\phi}_{H,L}^{(1)}(r) = \begin{pmatrix} 1 \\ 0 \end{pmatrix} r^{L+1} \quad \text{for} \quad r \to 0 \ , \tag{5.38}$$

$$\boldsymbol{\phi}_{H,L}^{(2)}(r) = \begin{pmatrix} 0 \\ 1 \end{pmatrix} r^{L+1} \quad \text{for} \quad r \to 0 \ , \tag{5.39}$$

such that the general solution of the homogeneous is

$$\boldsymbol{\phi}_{H,L}(r) = A_1 \boldsymbol{\phi}_{H,L}^{(1)}(r) + A_2 \boldsymbol{\phi}_{H,L}^{(2)}(r) \ . \tag{5.40}$$

We also find a particular solution of the inhomogeneous $\boldsymbol{\phi}_{I,L}(r)$ by iterating it at (5.32) with the initial condition for $r = \epsilon$

$$\boldsymbol{\phi}_{I,L}(r) = \begin{pmatrix} 1 \\ 0 \end{pmatrix} r^{L+1} \quad \text{for} \quad r \to 0 \ . \tag{5.41}$$

The full solution will be given by

$$\boldsymbol{\phi}_L(r) = \boldsymbol{\phi}_{I,L}(r) + A_1 \boldsymbol{\phi}_{H,L}^{(1)}(r) + A_2 \boldsymbol{\phi}_{H,L}^{(2)}(r) \ . \tag{5.42}$$

and is subject to the boundary condition at $r_{\max} >> d_x$

$$\boldsymbol{\phi}_L(r) = \begin{pmatrix} \chi_L(r) \\ u_L(r) \end{pmatrix} = \begin{pmatrix} i\, t_L\ h_L^{(1)}(kr) \\ b_L\ h_L^{(1)}(iqr) \end{pmatrix} kr \Bigg|_{r=r_{\max}} \ . \tag{5.43}$$

[4] formally, this comes from the asymptotic behaviour of a bound state wave function[38]: for a given energy $2\Delta m_S - E = q^2/(2\mu)$, the bound state solution is, asymptotically, $R_L(r) \approx h_L^{(1)}(iqr) \sim e^{(-qr)}$ for $r >> d$, *i.e.* it vanishes exponentially for $r \to \infty$

from which the coefficients A_1 and A_2 can be uniquely determined.

For doing so, one defines the logarithmic derivatives

$$\beta_L \equiv \frac{\mathrm{d}}{\mathrm{d}r}\log(\chi_L(r)) \tag{5.44}$$

$$= \frac{\chi'_{I,L} + A_1\chi'^{(1)}_{H,L} + A_2\chi'^{(2)}_{H,L}}{\chi_{I,L} + A_1\chi^{(1)}_{H,L} + A_2\chi^{(2)}_{H,L}} \ , \tag{5.45}$$

$$\gamma_L \equiv \frac{\mathrm{d}}{\mathrm{d}r}\log(u_L(r)) \tag{5.46}$$

$$= \frac{u'_{I,L} + A_1u'^{(1)}_{H,L} + A_2u'^{(2)}_{H,L}}{u_{I,L} + A_1u^{(1)}_{H,L} + A_2u^{(2)}_{H,L}} \ , \tag{5.47}$$

and use them to write continuity conditions on (5.43). They read

$$\beta_L = \left.\frac{h_L^{(1)}(kr) + rdh_L^{(1)}(kr)/dr}{rh_L^{(1)}(kr)}\right|_{r=r_{\max}} \ , \tag{5.48}$$

$$\gamma_L = \left.\frac{h_L^{(1)}(iqr) + rdh_L^{(1)}(iqr)/dr}{rh_L^{(1)}(iqr)}\right|_{r=r_{\max}} \ . \tag{5.49}$$

Equations (5.48) and (5.49) constitute a linear system of two equations with two unknown variables A_1 and A_2. Their algebraic solutions are

$$A_1 = -\frac{(\chi'_I - \beta_L\chi_I) - \Lambda_{H,2}(u'_I - \gamma_L u_I)}{(\chi'^{(1)}_H - \beta_L\chi^{(1)}_H) - \Lambda_{H2}(u'^{(1)}_H - \gamma_L u^{(1)}_H)} \ , \tag{5.50}$$

$$A_2 = -\frac{(\chi'_I - \beta_L\chi_I) - \Lambda_{H,1}(u'_I - \gamma_L u_I)}{(\chi'^{(2)}_H - \beta_L\chi^{(2)}_H) - \Lambda_{H,1}(u'^{(2)}_H - \gamma_L u^{(2)}_H)} \ , \tag{5.51}$$

where the abbreviation

$$\Lambda_{H,i} \equiv \frac{\chi'_{H,i} - \beta_L\chi_{H,i}}{u'_{H,i} - \gamma_L u_{H,i}} \tag{5.52}$$

was introduced and the index L was omitted for simplicity.

Finally, t_L can be extracted by using A_1 and A_2 in (5.40) and comparing it with (5.43) at $r_{\max}$ and the scattering phase-shift follows from (5.16).

5.4 Results and discussion

5.4.1 Wave-functions

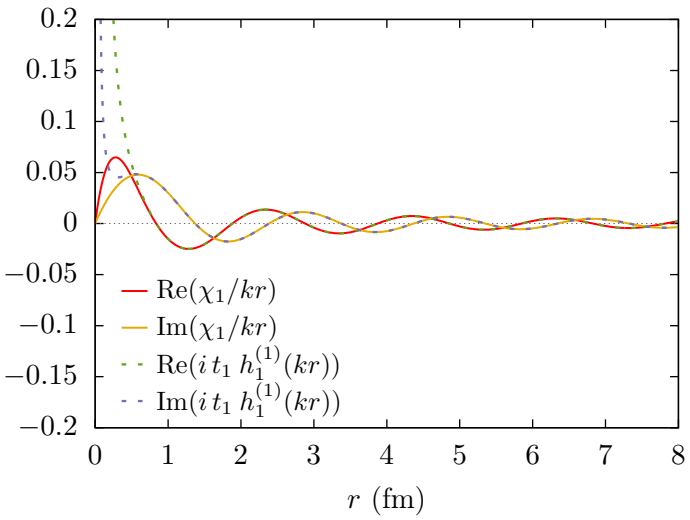

FIGURE 5.1: Radial wave functions χ/kr of the emergent wave in adimensional units as a function of r in comparison with the asymptotic condition for large r, the first order Hankel functions times it_1.

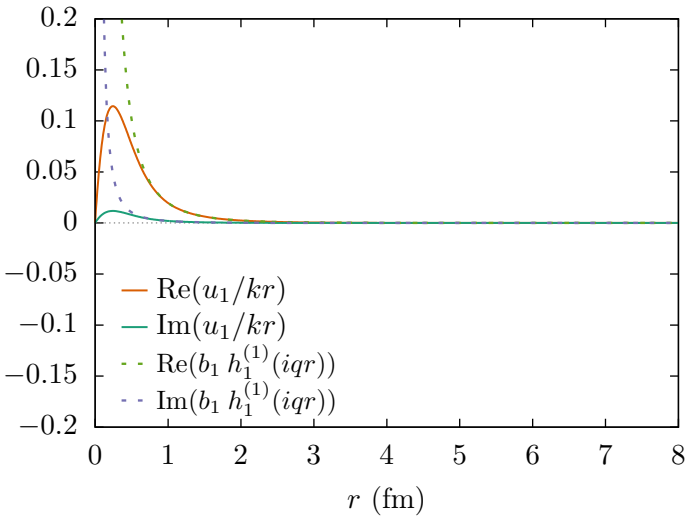

FIGURE 5.2: Radial wave functions u/kr of the bound state channel adimensional units as a function of r in comparison with the first order Hankel functions times b_1, which is the asymptotic condition for large r.

A plot of the emergent wave's radial wave functions is shown in Figure 5.1 and in adimensional units. The real and imaginary part of the emergent wave exhibit an out of phase oscillatory behaviour, with decreasing amplitude as a function of r. Starting

from $r \sim 1$ fm, they are consistent with an outgoing spherical wave emitted from a source at $r = 0$ (dashed lines). This is precisely the boundary conditions utilised here for large r. The bound state radial wave function is shown in 5.2. It peaks at $r \sim 0.3$ fm and decreases exponentially for large r, both for real and imaginary parts, being consistent with eigenfunctions of energy $q^2/2\mu$ bellow the threshold $2m_B*$. They also agree with the boundary condition for large r, shown in dashed lines. The agreements with the boundary conditions over a wide range of r gives a two-fold confirmation. The first is that we have obtained meaningful solutions to this adapted scattering problem, reflected by the appropriated choice of asymptotic boundary conditions[5]. Secondly, it confirms that the solutions are numerically stable over the range of $0 < r < 8$ fm.

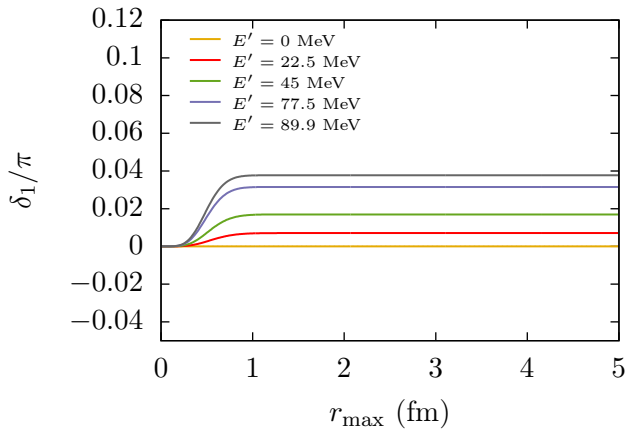

FIGURE 5.3: Plot of the phases shifts δ_1/π determined as function of the positions $r_{\max}$, where the asymptotic condition for large r is applied. We show the computation for five different energies in the interval $2m_B \leq E < 2m_B^*$, where in the plot $E' = E - 2m_B$ for shortness.

[5]In fact these boundary conditions rely on finite range potentials. Here, every potential term is a linear combinations of V_5, V_j. Each of them can be well treated as short ranged, because they scale with $\sim \mathrm{e}^{-r^2/d^2}$

5.4.2 Phase shifts

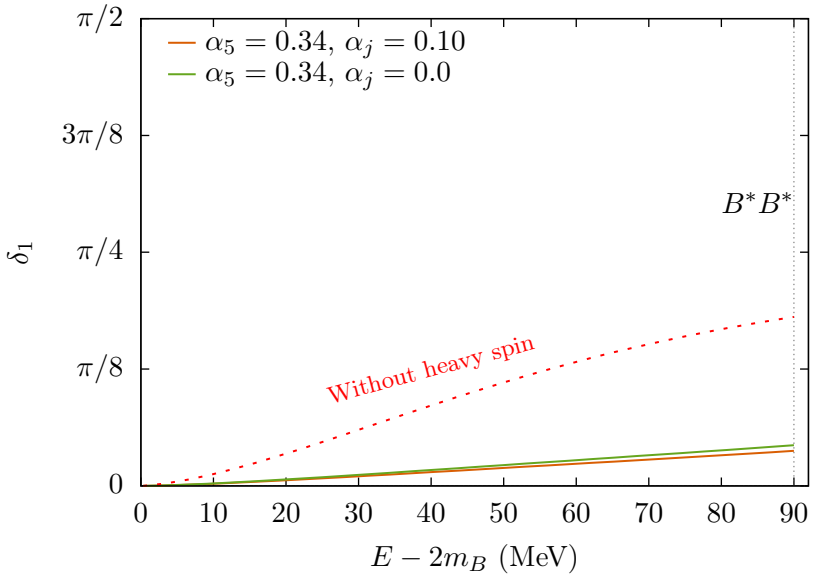

FIGURE 5.4: Phase shift δ_1 as a function of the system's energy eigenvalues $E-2m_{B^*}$ up to the $2m_{B^*}$ threshold. The orange continuous line shows the determination using the mean values of the $I = 0$ attractive potential V_5 and the repulsive V_j ($\alpha_5 = 0.34$, $d_5 = 0.45$ fm,$\alpha_j = 0.10$ $d_j = 0.28$ fm). The green continuous line corresponds to the artificial case where the repulsive V_j is null. Finally, the dashed red line gives the no-heavy-spin approximation, determined, for comparison, from a one-dimensional Schrödinger Equation with a single potential V_5, in according to [32]

Phase shifts were computed for the mean values of V_5 and V_j at $r_{\max} \approx 2$ fm up to to the B^*B^* threshold. From a stability analysis, presented in the plot of Figure 5.3, such values for $r_{\max}$ were shown to be sufficiently outside of the potentials' range, so that (5.36) applies. A plot as function of the system's energy can be seen in Figure 5.4. For comparison, we also computed the simpler case where heavy spins are disregarded [32] as well as the artificial case where the repulsive potential is null. It is seen that phase shifts seem to grow almost linearly with energy, both in the presence and in the absence of a repulsive potential, being very close to each other. They are both well bellow the values obtained disregarding heavy spins. There is no clear sign of resonances in the phase shifts, which would appear as an abrupt increase follow by a plateau.

It is also well-known that there are big uncertainties in the α and d parameters. In order to further access the influence of the potentials, phase shifts were also computed for increasing strength of the potentials. For doing so, values of α_5 up to 0.72 were used, keeping d_5 and d_j constant to preserve the scale. In order to increase α_j properly a strategy was followed, which is a rough estimate of α_j from α_5. It consists of considering the leading order perturbation theory determinations for attractive colour

triplet and repulsive colour sextet, are

$$V_5^{\text{pert}}(r) = -\frac{2\alpha_s}{3} r \ , \tag{5.53}$$

$$V_j^{\text{pert}}(r) = \frac{\alpha_s}{3} r \ , \tag{5.54}$$

where α_s is the QCD coupling constant. The comparison between (5.53) and (5.54) indicates that $\alpha_j \approx \alpha_5/2$. The new plots for the phase shifts are shown in Figure 5.5, including also the case where $V_j = 0$ in dashed lines. Once more, there is no clear sign of resonance. The phase shifts exhibit relevant increase starting from $\alpha_5 \sim 0.59$, that could indicate resonances, but even for $\alpha_5 = 0.72$ no plateau is reached up to the the threshold energy of B^*B^* pair mass, the limit of our analysis. This suggests that an analysis above this threshold could be required for a full picture. Further observations are that $\alpha_j = 0$ and $\alpha_j = \alpha_5/2$ provide very similar results, continuing to indicate that V_j does not play a strong influence in the scattered wave function. The shorter range of V_j when compared to V_5 ($d_j < d_5$) could be the reason for that, being the effective potential terms dominated by V_5.

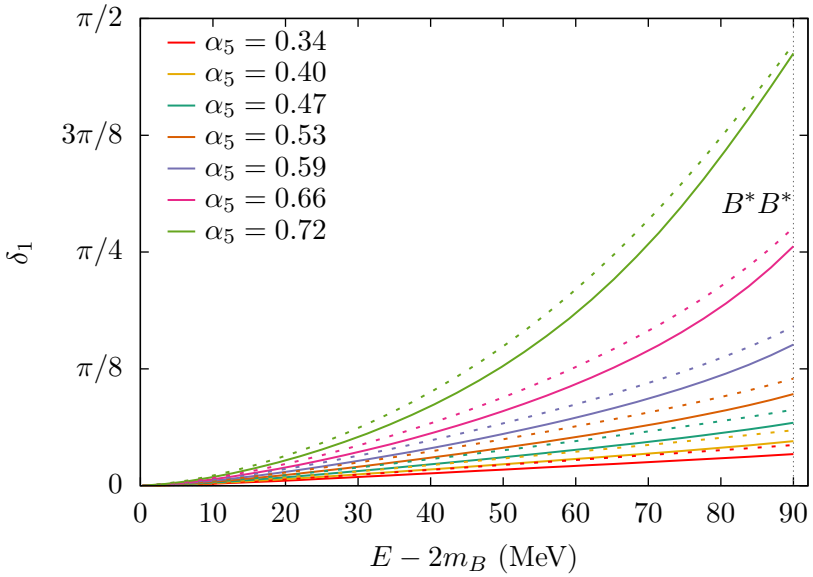

FIGURE 5.5: Phase shift δ_1 as a function of the system's energy eigenvalues $E - 2m_B^*$, up to the $2m_{B^*}$ threshold, for increasing strength of potentials. Couplings ranging from $0.34 \leq \alpha_5 \leq 0.72$ and $d_5 = 0.45$ fm and $d_j = 0.28$ fm are kept fixed to preserve the scales. Continuous line results from the computation using the approximation $\alpha_j = \alpha_5/2$, cf. (5.53) and (5.54). Dashed lines show the artificial case where the repulsive potential is null ($\alpha_j = 0$), for comparison.

5.4.3 Poles search in the second Riemann sheet

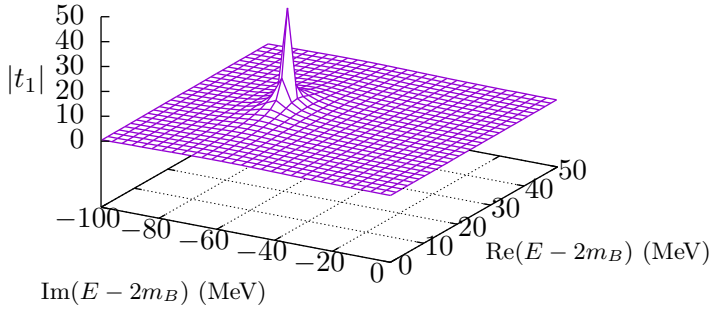

FIGURE 5.6: The eigenvalues t_1 as a function of the complex energy E, showing a pole at position $E - 2m_B \approx 17 - 56i$, calculated for a one-dimensional Schrödinger Equation with potential V_5, in according to [32]

Considering that the phase shifts did not provide a clear picture whether there are resonances or not, a further analysis was performed. It consists of searching for poles in the eigenvalues t_L of the matrix T. For doing so, equation (5.32) is solved for several complex energies. More specifically, a scan of t_L in a complex E grid is realised. When a clear sharp pole in t_L is found, its position in the real axis is related to the mass of the state

$$m = \mathrm{Re}(E - 2m_B) + 2m_B = \mathrm{Re}(E) \ . \tag{5.55}$$

and in the imaginary axes gives the decay width

$$\Gamma = -2\,\mathrm{Im}(E - 2m_B) = -2\,\mathrm{Im}(E) \ . \tag{5.56}$$

This type of strategy was already followed in a previous study [32] for a state with the same quantum numbers, but in the simpler case where heavy spins are not included. A clear pole was found. For comparison, this result is recovered here by solving the scattering problem of the 1×1 version of (5.32) [6] following exactly the same methods and numerical techniques used in the present work. A plot of $|t_1|$ in the complex plane for this case is shown in Figure 5.6. A sharp pole is present in the Second Riemann sheet with energy $E - 2m_B \approx 17 - 56i$ MeV, agreeing with the earlier results.

[6] for more details refer to [32]

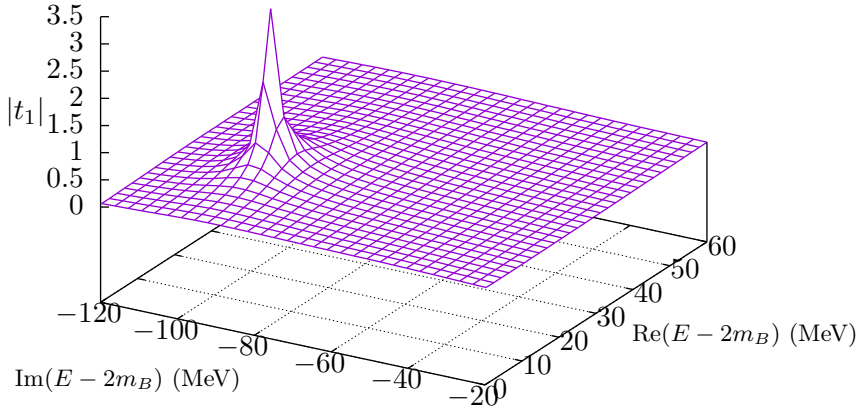

FIGURE 5.7: The absolute values of the eigenvalue t_1 as a function of the complex energy E for the present system using the mean values of the $I = 0$ of the potentials of the attractive V_5 and repulsive *i.e.* $\alpha_5 = 0.34$, $d_5 = 0.45$ fm,$\alpha_j = 0.10$ $d_j = 0.28$ fm. We use here $r_{\max} \approx 2.0$fm.

Next, the same procedure is applied for the system of interest (5.32). Figure 5.7 shows a plot of the corresponding $|t_1|$. A broader and weaker pole can be observed, further in the complex plane and with $E_{\text{pole}} \approx 20 - 95i$ MeV. Considering that, this time, the determination of t_1 in the complex plane has shown to be reasonably sensitive under changes in the numerical parameters, specially $r_{\max}$, which is not ideal, it is harder to state that the pole is not a mere result of numerical instabilities.

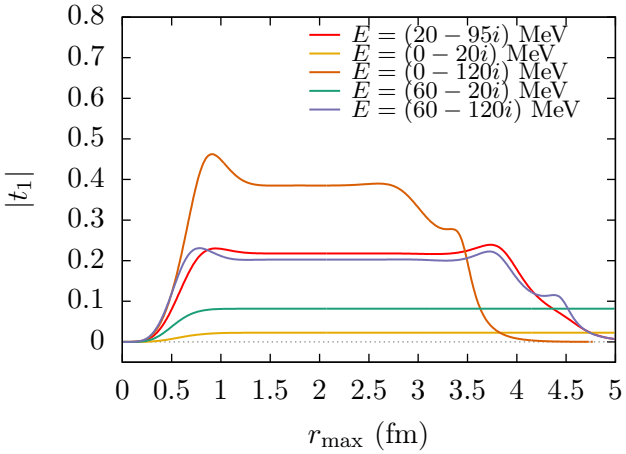

FIGURE 5.8: Stability analysis of $|t_1|$, plotted as a function of the positions $r_{\max}$ where the asymptotic condition for large r is applied. We present results for five different complex energies, four of which corresponds extremes of the grid in Figure 5.7 and one is supposedly close to the location of the pole in $|t_1|$.

In order to obtain a better comprehension, a closer stability analysis for t_1 was implemented. Figure 5.8 shows a plot of $|t_1|$ as a function of the choice of $r_{\max}$ in a range 0-5 fm, for five different values of complex energies, corresponding to the grid's four extremes and to a point close to the pole. It is observed that the stability of $|t_1|$ with respect to $r_{\max}$ depends on the complex energy eigenvalues. Common stability is achieved only for a small window $\sim$ 1.5-2.3 fm. This confirms that the values chosen for $r_{\max}$ to produce the plots in Figure 5.6 are in the stable region. On the other hand, the presence of a pole would give expectations of higher $|t_1|$ values for a energy $20 - 95i$ MeV, supposedly close to the pole, which is not the case. This could be due this energy not being close enough to the pole. However, further plots for energies in the surroundings produced similar results, hence this analysis was not conclusive. Even in the case of a physical pole, the state has shown a very small phase shift, with a pole located at a high imaginary energy. For this reason, results are suggesting that the resonance with quantum numbers $I(J^P)$ is suppressed by $\bar{b}\bar{b}$ spin effects.

Chapter 6

Conclusion and Outlook

This study has extended previous works by presenting a general formalism for the problem of including heavy spin corrections in the description of heavy light tetraquarks under the Born-Oppenheimer approximation using lattice QCD potentials . The framework demonstrates that, in order to preserve the wave functions' symmetries, the channels of B/B^* pair combinations allowed depend on the orbital angular quantum number L. More specifically, these channels are interchanged according to the parity of L, a manifestation of the Pauli Exclusion Principle in the system.

A coupled channel with quantum numbers corresponding to those of BB and B^*B^* meson pairs has been shown to be suitable for the search of a excited state with quantum numbers $I(J^P) = 0(1^-)$. A bound state analysis of such system with deliberate heavier than physical $\bar{b}\bar{b}$ masses offered insights to the effects of $\bar{b}$ spin in the system. They were responsible for a down shift in the system's binding energy, being the shift greater for lighter masses. Subsequently, an adaptation of the emergent wave method in order to consider a BB scattering channel coupled to a B^*B^* bound state channel has make possible an estimation of the BB scattering phase-shift. The phase-shift has been shown to decrease drastically when comparing to the approximation without heavy spin, as well as almost unaffected by the strength of the shorter-ranged repulsive potential of light spin $s_{qq} = 1$ and isospin $I = 0$.

An inspection of the scattering T matrix eigenvalues, t_L, in the complex plane was not conclusive, as the pole found is weak and fairly unstable with respect to the numerical parameters. Even in the hypothetical case of it being meaningful, its position in the imaginary energy axes would point to a very short-lived resonance, perhaps negligible. For further studies, a final investigation might need to be performed in order to determine the exact location of the pole. That could be done, for instance, via a complex root solver algorithm combined with a shooting method to search for roots in $1/t_1$. Next, a stability analysis of $|t_1|$ at the exact pole energy could reject the possibility of numeric instabilities. Finally, a further analysis that goes above the B^*B^* threshold would be interesting to rule out the possibility of a $I(J^P) = 0(1^-)$ resonance with energy above $2m_{B^*}$, providing a full picture of the system.

It is important to remark that this approach has a few limitations. On of them is related with the fact that heavy spins corrections are added asymptotically for large separations r, only, through the B/B^* ground state masses. As a result, couplings between orbital angular momentum and spin in such analysis are avoided. Secondly, in the current format of the Born-Oppenheimer approximation, orbital angular momentum is only assigned to the heavy degrees of freedom. For future studies, an evaluation of the spin-orbit effects and setting a Schrödinger equation with B/B^* masses, which, in turn, would be more evolved, could provide further interesting insights to the $ud\bar{b}\bar{b}$ spectra.

Bibliography

[1] M. Gell-Mann. "A schematic model of baryons and mesons". In: *Physics Letters* 8.3 (1964), pp. 214–215. ISSN: 0031-9163. DOI: https://doi.org/10.1016/S0031-9163(64)92001-3. URL: http://www.sciencedirect.com/science/article/pii/S0031916364920013.

[2] G Zweig. "An SU_3 model for strong interaction symmetry and its breaking; Version 2". In: CERN-TH-412 (Feb. 1964). Version 1 is CERN preprint 8182/TH.401, Jan. 17, 1964, 80 p. URL: http://cds.cern.ch/record/570209.

[3] R. J. Jaffe. "Multiquark hadrons. I. Phenomenology of $Q^2\overline{Q}^2$ mesons". In: *Phys. Rev. D* 15 (1 Jan. 1977), pp. 267–280. DOI: 10.1103/PhysRevD.15.267. URL: https://link.aps.org/doi/10.1103/PhysRevD.15.267.

[4] T. DeGrand et al. "Masses and other parameters of the light hadrons". In: *Phys. Rev. D* 12 (7 Oct. 1975), pp. 2060–2076. DOI: 10.1103/PhysRevD.12.2060. URL: https://link.aps.org/doi/10.1103/PhysRevD.12.2060.

[5] H. Miyazawa. "Reconnection of strings and quark matter". In: *Phys. Rev. D* 20 (11 Dec. 1979), pp. 2953–2959. DOI: 10.1103/PhysRevD.20.2953. URL: https://link.aps.org/doi/10.1103/PhysRevD.20.2953.

[6] M. Oka and C. J. Horowitz. "Hadron-hadron interaction in a string-flip model of quark confinement. II. Nucleon-nucleon interaction". In: *Phys. Rev. D* 31 (11 June 1985), pp. 2773–2779. DOI: 10.1103/PhysRevD.31.2773. URL: https://link.aps.org/doi/10.1103/PhysRevD.31.2773.

[7] M. Oka. "Hadron-hadron interaction in a string-flip model of quark confinement. I. Meson-meson interaction". In: *Phys. Rev. D* 31 (9 May 1985), pp. 2274–2287. DOI: 10.1103/PhysRevD.31.2274. URL: https://link.aps.org/doi/10.1103/PhysRevD.31.2274.

[8] F. Lenz et al. "Quark confinement and hadronic interactions". In: *Annals of Physics* 170.1 (1986), pp. 65–254. ISSN: 0003-4916. DOI: https://doi.org/10.1016/0003-4916(86)90088-6. URL: http://www.sciencedirect.com/science/article/pii/0003491686900886.

[9] S. Zouzou et al. "Four Quark Bound States". In: *Z. Phys. C* 30 (1986), p. 457. DOI: 10.1007/BF01557611.

[10] N. Brambilla et al. "QCD and strongly coupled gauge theories: challenges and perspectives". In: *The European Physical Journal C* 74.10 (Oct. 2014). ISSN: 1434-6052. DOI: 10.1140/epjc/s10052-014-2981-5. URL: http://dx.doi.org/10.1140/epjc/s10052-014-2981-5.

[11] N. K. Glendenning and J. Schaffner-Bielich. "Neutron star constraints on the H dibaryon". In: *Physical Review C* 58.2 (Aug. 1998), pp. 1298–1305. ISSN: 1089-490X. DOI: 10.1103/physrevc.58.1298. URL: http://dx.doi.org/10.1103/PhysRevC.58.1298.

[12] S.-K. Choi et al. "Observation of a Narrow Charmoniumlike State in ExclusiveBK+J/Decays". In: *Physical Review Letters* 91.26 (Dec. 2003). ISSN: 1079-7114. DOI: 10.1103/physrevlett.91.262001. URL: http://dx.doi.org/10.1103/PhysRevLett.91.262001.

[13] L. Maiani et al. "Diquark-antidiquark states with hidden or open charm and the nature ofX(3872)". In: *Physical Review D* 71.1 (Jan. 2005). ISSN: 1550-2368. DOI: 10.1103/physrevd.71.014028. URL: http://dx.doi.org/10.1103/PhysRevD.71.014028.

[14] B. Aubert et al. "Observation of a Broad Structure in the $\pi + \pi J/\Psi$ Mass Spectrum around 4.26 GeV/c^2". In: *Physical Review Letters* 95.14 (Sept. 2005). ISSN: 1079-7114. DOI: 10.1103/physrevlett.95.142001. URL: http://dx.doi.org/10.1103/PhysRevLett.95.142001.

[15] S. Coito and F. Giacosa. *On the origin of the $Y(4260)$*. 2020. arXiv: 1902.09268 [hep-ph].

[16] S.-K. Choi et al. "Observation of a Resonancelike Structure in the+Mass Distribution in ExclusiveBK+Decays". In: *Physical Review Letters* 100.14 (Apr. 2008). ISSN: 1079-7114. DOI: 10.1103/physrevlett.100.142001. URL: http://dx.doi.org/10.1103/PhysRevLett.100.142001.

[17] R. Aaij et al. "Observation of the Resonant Character of theZ(4430)State". In: *Physical Review Letters* 112.22 (June 2014). ISSN: 1079-7114. DOI: 10.1103/physrevlett.112.222002. URL: http://dx.doi.org/10.1103/PhysRevLett.112.222002.

[18] A. Bondar et al. "Observation of Two Charged Bottomoniumlike Resonances in(5S)Decays". In: *Physical Review Letters* 108.12 (Mar. 2012). ISSN: 1079-7114. DOI: 10.1103/physrevlett.108.122001. URL: http://dx.doi.org/10.1103/PhysRevLett.108.122001.

[19] M. Ablikim et al. "Observation of a Charged Charmonium like Structure in$e + e \to \pi + \pi J/\Psi$ at 4.26 GeV". In: *Physical Review Letters* 110.25 (June 2013). ISSN: 1079-7114. DOI: 10.1103/physrevlett.110.252001. URL: http://dx.doi.org/10.1103/PhysRevLett.110.252001.

[20] LHCb collaboration et al. *Observation of structure in the J/ψ-pair mass spectrum*. 2020. arXiv: 2006.16957 [hep-ex].

[21] S. Prelovsek et al. "Study of theZc+channel using lattice QCD". In: *Physical Review D* 91.1 (Jan. 2015). ISSN: 1550-2368. DOI: 10.1103/physrevd.91.014504. URL: http://dx.doi.org/10.1103/PhysRevD.91.014504.

[22] P. Bicudo and M. Cardoso. *Tetraquark bound states and resonances in the unitary and microscopic triple string flip-flop quark model, the light-light-antiheavy-antiheavy $qq\bar{Q}\bar{Q}$ case study*. 2015. arXiv: 1509.04943 [hep-ph].

[23] A. V. Manohar and M. B. Wise. "Exotic states in QCD". In: *Nuclear Physics B* 399.1 (June 1993), pp. 17–33. ISSN: 0550-3213. DOI: 10.1016/0550-3213(93)90614-u. URL: http://dx.doi.org/10.1016/0550-3213(93)90614-U.

[24] B. Silvestre-Brac and C. Semay. "Spectrum and decay properties of diquonia". In: *Z. Phys. C - Particles and Fields* 59 (Sept. 1993), pp. 457–470. ISSN: 5850949. DOI: 10.1007/BF01498626. URL: https://doi.org/10.1007/BF01498626.

[25] C. Michael and P. Pennanen. "Two heavy-light mesons on a lattice". In: *Physical Review D* 60.5 (July 1999). ISSN: 1089-4918. DOI: 10.1103/physrevd.60.054012. URL: http://dx.doi.org/10.1103/PhysRevD.60.054012.

[26] J. Vijande, A. Valcarce, and K. Tsushima. "Dynamical study of QQ–$\bar{u}\bar{d}$mesons". In: *Physical Review D* 74.5 (Sept. 2006). ISSN: 1550-2368. DOI: 10.1103/physrevd.74.054018. URL: http://dx.doi.org/10.1103/PhysRevD.74.054018.

[27] S.-Q. Luo et al. "Exotic tetraquark states with the $qq\bar{Q}\bar{Q}$ configuration". In: *The European Physical Journal C* 77.10 (Oct. 2017). ISSN: 1434-6052. DOI: 10.1140/epjc/s10052-017-5297-4. URL: http://dx.doi.org/10.1140/epjc/s10052-017-5297-4.

[28] Z. S. Brown and K. Orginos. "Tetraquark bound states in the heavy-light heavy-light system". In: *Physical Review D* 86.11 (Dec. 2012). ISSN: 1550-2368. DOI: 10.1103/physrevd.86.114506. URL: http://dx.doi.org/10.1103/PhysRevD.86.114506.

[29] P. Bicudo and M. Wagner. "Lattice QCD signal for a bottom-bottom tetraquark". In: *Physical Review D* 87.11 (June 2013). ISSN: 1550-2368. DOI: 10.1103/physrevd.87.114511. URL: http://dx.doi.org/10.1103/PhysRevD.87.114511.

[30] P. Bicudo et al. "BB interactions with static bottom quarks from lattice QCD". In: *Physical Review D* 93.3 (Feb. 2016). ISSN: 2470-0029. DOI: 10.1103/physrevd.93.034501. URL: http://dx.doi.org/10.1103/PhysRevD.93.034501.

[31] P. Bicudo, J. Scheunert, and M. Wagner. "Including heavy spin effects in the prediction of a $\bar{b}\bar{b}ud$ tetraquark with lattice QCD potentials". In: *Physical Review D* 95.3 (Feb. 2017). ISSN: 2470-0029. DOI: 10.1103/physrevd.95.034502. URL: http://dx.doi.org/10.1103/PhysRevD.95.034502.

[32] P; Bicudo et al. "$ud\bar{b}\bar{b}$ tetraquark resonances with lattice QCD potentials and the Born-Oppenheimer approximation". In: *Physical Review D* 96.5 (Sept. 2017). ISSN: 2470-0029. DOI: 10.1103/physrevd.96.054510. URL: http://dx.doi.org/10.1103/PhysRevD.96.054510.

[33] P. Bicudo et al. "Evidence for the existence of $ud\bar{b}\bar{b}$and the nonexistence of $ss\bar{b}\bar{b}$ and $cc\bar{b}\bar{b}$ tetraquarks from lattice QCD". In: *Physical Review D* 92.1 (July 2015). ISSN: 1550-2368. DOI: 10.1103/physrevd.92.014507. URL: http://dx.doi.org/10.1103/PhysRevD.92.014507.

[34] M. Fierz. "Zur Fermischen Theorie des -Zerfalls". In: *Zeitschrift für Physik* 104 (1937), pp. 553–565.

[35] R. H. Good. "Properties of the Dirac Matrices". In: *Rev. Mod. Phys.* 27 (2 Apr. 1955), pp. 187–211. DOI: 10.1103/RevModPhys.27.187. URL: https://link.aps.org/doi/10.1103/RevModPhys.27.187.

[36] C. C. Nishi. "Simple derivation of general Fierz-type identities". In: *American Journal of Physics* 73.12 (Dec. 2005), pp. 1160–1163. ISSN: 1943-2909. DOI: 10.1119/1.2074087. URL: http://dx.doi.org/10.1119/1.2074087.

[37] J. Scheunert. "Combining Lattice QCD results and Nonrelativistic Quantum Mechanics in the Born-Oppenheimer Approximation to study possibly existing Tetraquarks". MA thesis. Max-von-Laue-Str. 1, 60438 Frankfurt am Main, Germany: Institut für Theoretische Physik der Goethe-Universität Frankfurt, 2015. URL: https://itp.uni-frankfurt.de/~mwagner/theses/MA_Scheunert.pdf.

[38] E. Merzbacher. *Quantum mechanics*. English. 3 ed. J. Wiley New York, 1998.

[39] R. G. Gordon. "New Method for Constructing Wavefunctions for Bound States and Scattering". In: *The Journal of Chemical Physics* 51.1 (1969), pp. 14–25. DOI: 10.1063/1.1671699. URL: ttps://doi.org/10.1063/1.1671699.

[40] "Coupled channel methods for solving the bound-state Schrödinger equation". In: *Computer Physics Communications* 84.1 (1994), pp. 1–18. ISSN: 0010-4655. DOI: https://doi.org/10.1016/0010-4655(94)90200-3. URL: http://www.sciencedirect.com/science/article/pii/0010465594902003.

[41] Z. Bačić and J. C. Light. "Theoretical Methods for Rovibrational States of Floppy Molecules". In: *Annual Review of Physical Chemistry* 40.1 (1989), pp. 469–498. DOI: 10.1146/annurev.pc.40.100189.002345. URL: https://doi.org/10.1146/annurev.pc.40.100189.002345.

[42] P. Bicudo et al. "Bottomonium resonances with $I = 0$ from lattice QCD correlation functions with static and light quarks". In: *Physical Review D* 101.3 (Feb. 2020). ISSN: 2470-0029. DOI: 10.1103/physrevd.101.034503. URL: http://dx.doi.org/10.1103/PhysRevD.101.034503.

[43] E. Eichten and B. R. Hill. "Static effective field theory: 1/m Corrections". In: *Phys. Lett. B* 243 (1990), pp. 427–431. DOI: 10.1016/0370-2693(90)91408-4.

[44] M. Neubert. "Heavy-quark symmetry". In: *Physics Reports* 245.5-6 (Sept. 1994), pp. 259–395. ISSN: 0370-1573. DOI: 10.1016/0370-1573(94)90091-4. URL: http://dx.doi.org/10.1016/0370-1573(94)90091-4.

[45] A. S. Kronfeld and J. N. Simone. "Computation of $\bar{\Lambda}$ and λ_1 with lattice QCD ". In: *Phys. Lett. B* 490 (2000), pp. 228–235. DOI: 10.1016/S0370-2693(00)00833-9. arXiv: hep-ph/0006345.

[46] William H. Press et al. *Numerical Recipes 3rd Edition: The Art of Scientific Computing*. 3rd ed. USA: Cambridge University Press, 2007. ISBN: 0521880688.

[47] George G. *An Essay on the Application of mathematical Analysis to the theories of Electricity and Magnetism*. 1828. arXiv: 0807.0088 [physics.hist-ph].

[48] W.E. Boyce, R.C. DiPrima, and D.B. Meade. *Elementary Differential Equations and Boundary Value Problems*. Wiley, 2017. ISBN: 9781119443766.

Acknowledgements

I acknowledge the "Goethe Goes Global" Scholarship Program for the funding of my master. I would like to express my gratitude to Prof. Dr. Marc Wagner, supervisor and mentor, for his great availability for discussions and for substantial support provided along the program. I am also grateful to the smart Jakob Hoffmann, for his big interest in the project, resulting in useful discussions and pleasurable collaborations. I would like to thanks Martin Pflaumer, Jonnas Scheunert, for helpful clarifications on previous works, and Lasse Müller for interest in the project. Additionally, I am also deeply thankful to all my friends that provided contributions: between them, Emanuele Di Maio, for important feedback given to the presentation; Vicenzo Ventriglia, for helpful advises; Angela Opatz, for the support in stress times... Finally, I would like to immensely thank my family, which is always supporting me in the pursue of my dreams, even when they involve $\sim 1/4$ of earth's circumference distances.